

Stellar Populations

Reynier Peletier
(Kapteyn Astronomical Institute)
University of Groningen,
Postbus 800, 9700 AV Groningen,NL

(To appear in XXIII Canary islands winter school of astrophysics
ed. J. Falcón-Barroso & J.H. Knapen)

September 21, 2018

Abstract

This is a summary of my lectures during the 2011 IAC Winter School in Puerto de la Cruz. I give an introduction to the field of stellar populations in galaxies, and highlight some new results. Since the title of the Winter School was *Secular Evolution in Galaxies* I mostly concentrate on nearby galaxies, which are best suited to study this theme. Of course, the understanding of stellar populations is intimately connected to understanding the formation and evolution of galaxies, one of the great outstanding problems of astronomy. We are currently in a situation where very large observational advances have been made in recent years. Galaxies have been detected up to a redshift of 10. A huge effort has to be made so that stellar population theory can catch up with observations. Since most galaxies are far away, information about them has to come from stellar population synthesis of integrated light. Here I will discuss how stellar evolution theory, together with observations in our Milky Way and Local Group, are used as building blocks to analyze these integrated stellar populations.

Contents

| | | |
|-------|--|----|
| 1.1 | Introduction | 2 |
| 1.2 | A quick look at galaxy images | 5 |
| 1.3 | Stellar population models and their ingredients | 7 |
| 1.3.1 | Stellar evolution theory | 10 |
| 1.3.2 | Stellar libraries | 12 |
| 1.3.3 | The Initial Mass Function | 14 |
| 1.3.4 | Abundance ratios | 15 |
| 1.4 | Stellar population analysis of individual galaxies | 18 |
| 1.4.1 | The age-metallicity degeneracy and luminosity weighting | 18 |
| 1.4.2 | Analysis using colors, and the role of extinction | 20 |
| 1.4.3 | Analysis using optical spectra | 26 |
| 1.4.4 | Star Formation Histories and the SSP | 31 |
| 1.4.5 | Learning about stellar populations using 2D spectroscopy | 32 |
| 1.4.6 | Stellar masses and the IMF in galaxies | 34 |
| 1.4.7 | Beyond the optical | 39 |
| 1.4.8 | Stellar population analysis from surface brightness fluctuations | 41 |
| 1.5 | The use of scaling relations | 43 |
| 1.5.1 | The color – σ relation | 43 |
| 1.5.2 | Stellar Population Analysis from Spitzer Colors | 46 |
| 1.5.3 | The fundamental plane of galaxies | 49 |
| 1.6 | Stellar Population gradients in early-type galaxies | 55 |
| 1.7 | Future prospects | 57 |

1.1 Introduction

We are living in an era in which we are able to see the light of galaxies at or close to redshift 10. Many galaxies above a redshift of 3 are already known, and we are starting to discover their clustering properties. These galaxies must undergo an evolution which leads to the galaxies we see around us, of which we have catalogues containing millions of individuals. Understanding how this evolution has taken place is a major task that the current generation of astronomers will have to address. A major tool needed to study galaxy evolution is stellar population synthesis. At high redshift galaxy are not more than point sources

of which we can measure the flux in one or more bands, or a spectrum, if we are lucky. The information contained in such a spectrum can, however, be very powerful. It can tell us how old the stars are that emit the light that we see, and give us some clues about their internal composition. This information, together with spatial information about the distribution of galaxies, and information about the gas content of these objects, is crucial input for large galaxy formation simulations, which try to simulate the formation and evolution of galaxies in the Universe.

To interpret the fluxes and spectra of high redshift galaxies, we need models that tell us how stellar populations evolve as a function of time. With them, we can then use the fact that astronomers can look back in time, to determine a 3D movie of the evolution of galaxies in the Universe. Even some predictions can be made about the future. Such models are best made using the detailed information around us, from the Sun, which shows us in detail how one particular star evolves, to other stars, to galaxies in the Local Group, which we can resolve into individual stars, to galaxies in the local Supercluster, for which we can obtain important spatial information. Stellar population models have been built on knowledge from many different fields, and are continuously improving in quality, as our understanding of many physical processes improves, the capacity of our computers increases, and our instruments and telescopes become larger and better.

Research on stellar populations is relatively old. In the beginning of the 20th century the Hertzsprung-Russell diagram was discovered, i.e., the relation between the color and luminosity of stars. The HR diagram showed that stars evolve in an ordered way. Shapley (1918) could show from Cepheids that globular clusters are large systems of stars at several kpc from us centered around a point which later became known as the center of our Galaxy. Soon afterwards, it was found that nebulae such as M31 were even larger systems than globular clusters (galaxies) much further away. It was realized by Baade (1944) that some regions of M31 were similar to our Galactic disk as far as the kind of stars present were concerned, and that the bulge of M31 looked like our Galactic halo. As a result, one realized that the variation of properties along Hubble's galaxy classification sequence was strongly connected with star formation in galaxies. Early works studying galaxy colors to derive information about their stellar contents were by Stebbins, Whitford, Holmberg, Humason, Mayall, Sandage, Morgan, and de Vaucouleurs (see Whitford 1975 for a summary of the early work in this field). A nice review about the known galaxy properties is given by Roberts (1963). Roberts' analysis established the basic elements of our current picture of the Hubble sequence as a monotonic sequence in present-day SFRs and past star formation histories.

To go further than recognizing differences between galaxies, and to be able to give quantitative predictions for stellar populations in galaxies that can be tested with real data, a paradigm of evolutionary stellar population models was developed by Tinsley (1968, 1980, etc.). In Kennicutt (1999) the importance of Tinsley's stellar population work has been summarized. She developed a methodology for constructing evolutionary synthesis models for colors, gas con-

tents and chemical abundances with time, heavily influenced by the ideas about galaxy formation published in 1963 by Eggen, Lynden-Bell & Sandage (1962). This *evolutionary synthesis* paradigm, which is still being used by our current, most sophisticated models, needs input from stellar evolution calculations, nucleosynthesis models, and cosmological models, and is made to fit the observed colors and magnitudes of stars and galaxies, as well as their line strengths. An important result of her models was that she was able to describe the evolution of colors and magnitudes along the Hubble Sequence as a function of one parameter, which could be M/L ratio, gas fraction or age. A second result was that the luminosity evolution of passive galaxies was much larger than had been estimated earlier. Before her work it was claimed that one could constrain q_0 and Λ from the evolution of magnitudes and colors. However, nowadays one knows that the evolution due to aging and other population effects is so large compared to effects of cosmological signatures that this method is not very useful. Because she was able to indicate the importance of stellar population research, Tinsley became the focal point of galaxy evolution research and a role model for younger scientists. The conclusion from her work was that galaxy evolution was an observable phenomenon (see Kennicutt 1999).

Tinsley's ideas were incorporated into the models of Faber (1972), and of Searle, Sargent & Bagnulo (1973), who also added a parameterization for the Star Formation History. For a number of years people seriously tried to compete with these evolutionary models using *empirical* models that did not need any input from theory (e.g. O'Connell 1980, Bica 1988), but these efforts have died out, since it is hard to learn much about the evolution of stellar populations in this way.

Since the time of Tinsley, our observing capacity has improved enormously. We have CCDs, linear devices that make it possible to record accurately images and spectra of galaxies. Telescopes have increased in size, but, more importantly, the Hubble Space Telescope has caused a revolution in the field of stellar populations. The high spatial resolution, the long integrations, and the changing paradigm to work with sometime very large, surveys, has made it possible to obtain high S/N data of very far away galaxies, and at the same time very high quality, detailed images of nearby objects. Such images become even more powerful in the presence of the large SDSS survey, which makes it possible to carefully select galaxies for detailed studies using HST. Also very important, compared to Tinsley's time, is that we have started to explore most of the electromagnetic spectrum, and also non-baryonic matter. Knowing about the huge presence of dark matter completely changes our idea about the expansion of the Universe and the interactions between galaxies, and is therefore crucial to understand galaxy evolution.

Fig. 1.1, from Brinchmann (2010) indicates some very basic problems in our field, which will hopefully be solved in the coming decades. On the left the morphology-density relation by Dressler (1980). Understanding why in clusters in the local Universe the fraction of early-type galaxies, both dwarfs and giants, is so much larger than in the field, is a fundamental question, which needs full attention of our community. Then in the middle the mass metallicity relation.

This relation is one of the most fundamental relations in the field of galaxy formation and evolution. The solution depends on how a galaxy is formed from the primordial gas, on feedback at all times, on interaction with its environment, and on many other things. And on the left the dichotomy in the mass – D_{4000} relation, which loosely can be called the mass – age relation. It is clear that smaller galaxies form their stars later. Why is this, and why is there a distinct break?

The contents of this review will be the following. I will start with a quick look at galaxy images, so that the reader can get a feeling of the different stellar populations (Section 1.2). After that I will discuss various aspects of Stellar Population Models (Section 1.3), such as stellar evolution theory, stellar libraries, the Initial Mass Function and abundance ratios. In the next Section (1.4 I will discuss stellar population analysis of individual galaxies, using colors and spectra, in the optical and elsewhere. I will discuss obtaining star formation histories, and end this section with a few words on surface brightness fluctuations. Following this, in Section 1.5 I will discuss stellar population analysis using scaling relations with ensembles of galaxies. In Section 1.6 radial gradients in the galaxies will be discussed. I will end with some prospects for the future.

1.2 A quick look at galaxy images

In 1943, aided by the blackout in Pasadena caused by the second world war, Baade for the first time was able to resolve M31 and its companions into individual stars (Baade 1944). Realizing that the stellar populations in NGC 205 and M 32 are similar to the stars in globular clusters in our Galaxy, Baade recognized that stellar populations fall into 2 groups: Population I stars, which look like the stars in the solar neighborhood, and Population II stars, which are similar to those in globular clusters. Characteristic for Population I are high luminosity O and B stars, as well as open clusters. Characteristic for Population II are short-period Cepheids. Early-type galaxies, according to him, only contained Population II, while in late and intermediate-type galaxies a mix of both populations was found. Only much later on (in the 1970 and 1980's by Whitford (1978), Whitford & Rich (1983), Rich (1988), Terndrup (1988), etc.) it was found that these stars were very different, with bulge stars being metal rich, while halo stars are very metal poor. Both populations, on the other hand, have in common that they do not contain any blue giant stars.

At present, we think that our Galaxy contains several components: the rotating (thin) disk with population I stars, the thick disk (Gilmore & Reid 1983), the stellar halo and the Galactic bulge. In the halo several globular clusters are found. Some others have properties more like the thin disk and are therefore called disk globular clusters (Zinn & West 1984).

We are in the lucky situation that now with the Hubble Space Telescope we can imitate Baade's observations for galaxies up to about 10 Mpc, i.e. a factor 50 further away. The Hubble Legacy Archive (<http://hla.stsci.edu/>) offers fantastic images enabling everybody to *observe* galaxies at a resolution which is

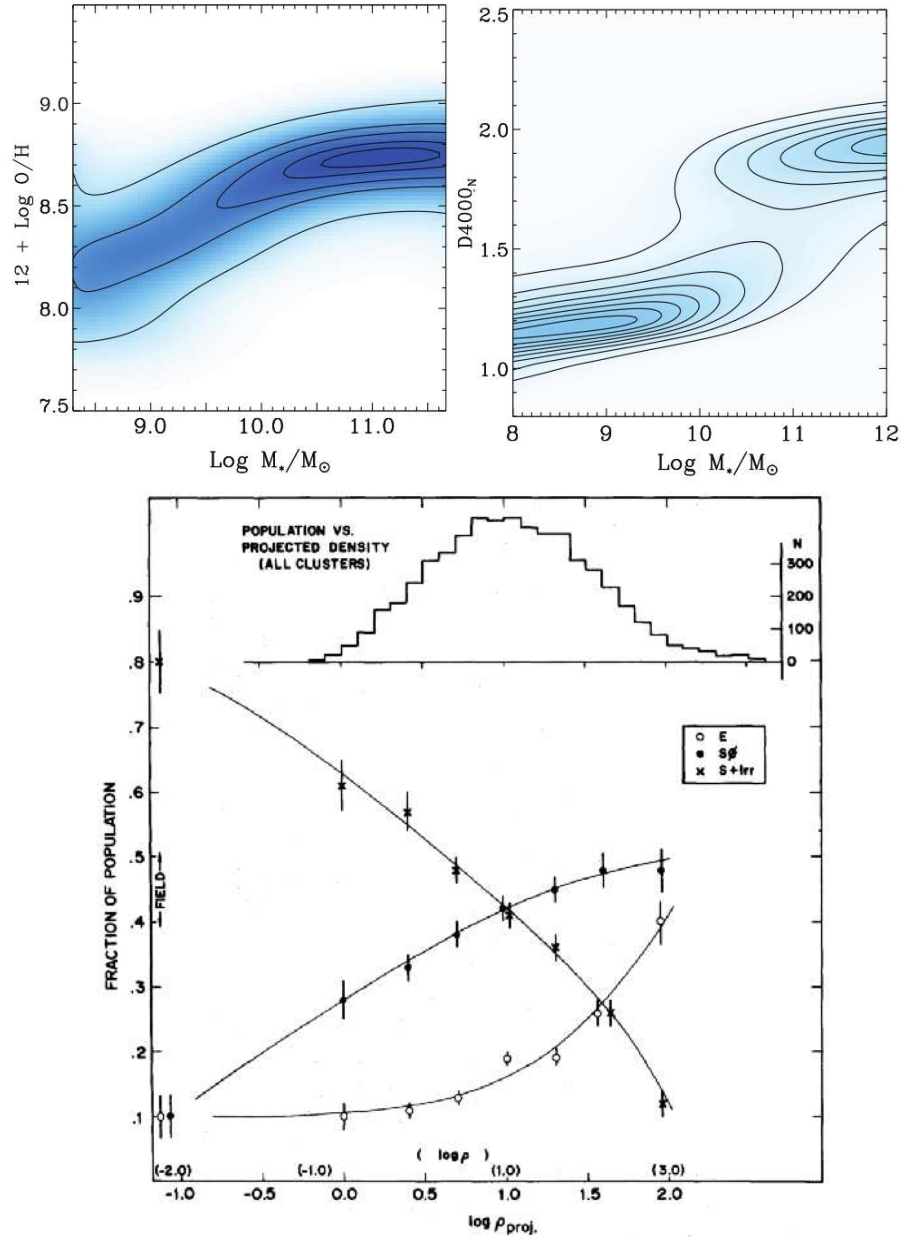


Figure 1.1: On the top left is shown the mass-metallicity relation for SDSS DR6 (Tremonti et al. 2004). Top right: The relation between stellar mass and the 4000Å break in the SDSS DR7 (Kauffmann et al. (2003)). These figures have been reproduced from Brinchmann (2010). Bottom panel: On the left the Morphology-Density relation (Dressler 1980), showing the strong relation between the galaxy density and the fraction of early-type galaxies.

a factor 10 better than one can get from the ground. As was the case for me, when I was an undergraduate student in Leiden in the 1980's when I studied the Palomar Sky plates: it is extremely instructive to look at images of the Universe. For example, by simply studying maps of galaxy clusters such as Virgo or Coma one gets a very good idea of the morphology-density relation. I will show here the galaxy M51 at 8 Mpc. Taking the composite F814W/F555W/F435W image one clearly sees the spiral arms, the dust lanes, the position of star forming regions close to the dust lanes, etc. (Fig. 1.2). Zooming in into the area marked with a red cross one sees a large star forming complex in the spiral arm (Fig. 1.2(right)), together with many small and large dust lanes. Zooming in one step further into the star forming complex (Fig. 1.3(left)) one sees the red and blue (super)giants individually resolved. The stellar populations here are similar to a young open cluster, containing both young and old stars. Outside the spiral arm (Fig. 1.3(right)) fewer stars are being seen. The brightest stars have disappeared, both the blue and the red ones, and the stellar population appears to be much more uniform than in the spiral arm. Here one barely resolves the brightest red giants of a stellar population, which looks similar to Population II.

A factor of 2 in distance further from us, we can still resolve individual stars with the Hubble Space Telescope. In the Coma cluster, however, another factor of 6 further away, this is not possible any more. Here information about individual stars can still be obtained using surface brightness fluctuations (see subsection 1.4.8), analyzing the statistics of the light in individual pixels. When going even further away the only way to derive information about stellar populations in galaxies is by analyzing the integrated light. In most of this paper we will discuss ways to do this, and the results that are obtained.

1.3 Stellar population models and their ingredients

With stellar population synthesis one wants to determine as much information from the stellar populations of an unresolved galaxy from a single spectrum as possible. Having seen how complicated our Milky Way is, it is clear that one cannot retrieve all the information that one would like to have. The integrated light contains contributions from stars with a large range in metallicity, mass and age, and even for stars of a fixed metallicity the relative distribution of elements might be different from one star to another. Since all this together is too much to obtain from a single spectrum, one often assumes an *Initial Mass Function (IMF)*, the number of stars per mass interval at the moment that the stars were born, and tries to derive the star formation history (SFH) and the metallicity distribution of the stars in a galaxy.

The spectrum of an integrated stellar population is obtained by integrating all stars along the line of sight.

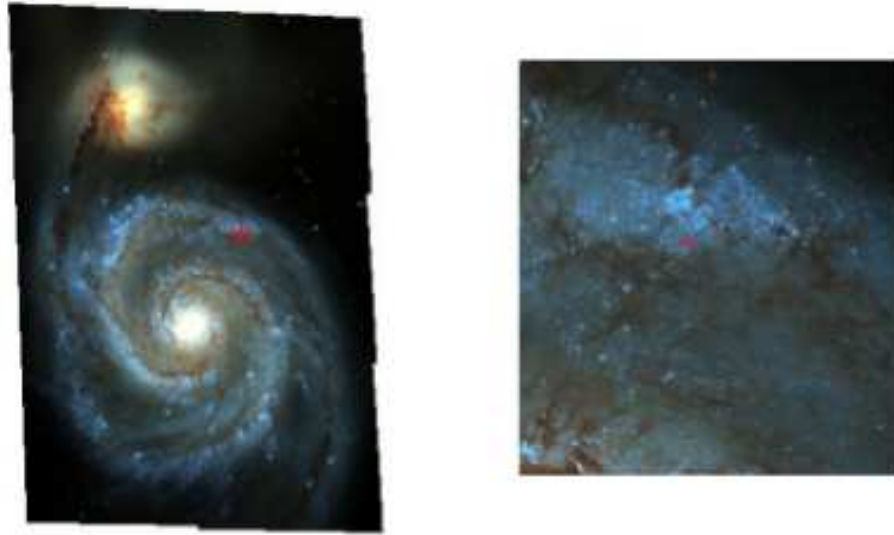


Figure 1.2: Left: Composite HST F814W/F555W/F435W image of M 51 (from the Hubble Legacy Archive). Right: Zoom at the position of the cursor, showing the stellar populations around a spiral arm.

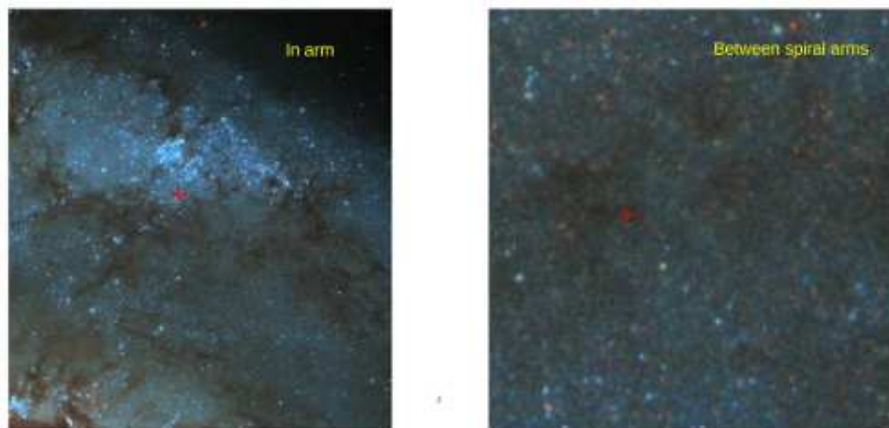


Figure 1.3: Magnifications of Fig. 1.2 in (left) and out of the spiral arm (right). Note the enormous difference in resolved stellar populations.

$$S_\lambda(t, Z) = \int_{m_{\text{low}}}^{m_{\text{up}}} S_\lambda(m, t, Z) N(m) F(m, t, Z) dm \quad (1.1)$$

Here $S_\lambda(m, t, Z)$ is the spectral energy distribution (SED) of a star of mass m (going from m_{up} to m_{low}), age t and metallicity Z , and $F(m, t, z)$ the flux in a normalizing band. The total galaxy spectrum is then obtained by adding the contributions of the various ages and metallicities.

Modern stellar population synthesis assumes that the stellar populations in galaxies consist of a sum of *Single Stellar Populations (SSP)*, building blocks of more complex stellar populations, entities that consist of all stars born at the same time, with the same metallicity. For example, galaxies do not consist only of A-stars of 2 solar mass, but stars of the full range of masses in the range of the IMF must exist. With this strong assumption, one can use stellar evolution theory to calculate the integrated properties of these SSPs, and then decompose the SED of galaxy into various SSPs. Justification of the SSP approach dates back from the time of Tinsley, who realized that clusters, both globular and open, could all be represented as single stellar populations. When looking at the nearest galaxies, the SSP approximation remains valid (Section 1.4.2). A nice overview of evolutionary stellar population models is given by Maraston (2005). Current SSP models predict full spectral energy distributions (SEDs) by integrating stellar spectra along theoretical isochrones. These spectra are selected from a stellar library, that consist of observations of real stars or of artificial spectra calculated using model atmospheres. Some of the presently most popular stellar population models are those by Worthey (1994), Maraston (2005), Bruzual & Charlot (2003) and later unpublished versions, Le Borgne et al. 2004 (Pégase HR), Leitherer et al. 2010 (Starburst99), Vazdekis et al. (2010), González Delgado et al. (2005) and Schiavon (2007).

Despite important progress in the last 2 decades, it is still not straightforward to routinely derive star formation histories and metallicity distributions from spectra. Here I will briefly indicate a number of reasons why this is the case, and in the coming sections I will elaborate on them. First of all, there is our relatively poor understanding of the advanced phases of stellar evolution, such as the supergiant phase and the asymptotic-giant-branch (AGB) phase. Stars in these phases are bright and short lived, so that they do contribute significantly to the spectrum of galaxies, but their numbers in color-magnitude diagrams of globular and open clusters are not large enough to constrain the fraction of light of these populations in the total spectrum. At the same time, mass loss, which is difficult to model, and is crucial for calculating their evolutionary path, plays such an important role in these stars, that it causes considerable uncertainties. Stars on the AGB contribute especially in the infrared, and in this region especially these uncertainties are most important.

A second, also very important problem is the age-metallicity degeneracy. In an integrated stellar population, the main effect of increasing the metallicity is raising the opacities of stars on the red giant branch (RGB), causing it to become redder, which implies that the integrated spectrum is redder, and that

most strong atomic features in the optical are stronger, since they are stronger in cooler stars. The main effect of increasing the age is the same: the reddening of the RGB. This means that one can often not derive both age and metallicity at the same time: the so-called age-metallicity degeneracy. This degeneracy in fact can get worse: if there is dust in the galaxy, it will cause colors to become redder, acting in the same way as increasing metallicity or age. However, only colors are strongly affected by the effects of dust extinction. Line strengths are mostly not affected by extinction, except if blue and red continuum are lying very far away from each other. As a result, ages and metallicities are strongly degenerate, although there are ways to measure both parameters separately.

A third problem is that abundance ratios of galaxies are not always the same as in the solar neighborhood. This shows up in our Galaxy as a tight relation of $[\text{Mg}/\text{Fe}]$ and metallicity $[\text{Fe}/\text{H}]$ (Edvardsson et al. 1993). It is thought that element formation is mainly taking place in supernovae of type Ia and II. In explosions of SN type II (massive stars) the amount of O and other α -elements, as compared to Fe, that is produced is much larger than in SN of type Ia. It is believed that during the formation of halo and bulge the number of SN type II relative to type Ia was much higher than during the formation of the disk, and as a result the ratio of Mg/Fe abundance is higher in our Galactic halo and bulge than in the Galactic disk. Not only does the fraction of α -elements relative to Fe vary. Variations are also seen in the ratio of other elements to Fe (see the review of Henry & Worthey 1999). At present stellar population models (both the stellar isochrones and the stellar libraries) rarely contain abundance distribution other than solar. This means that several features in observed galaxy spectra are not well fit by the best currently available stellar population models.

1.3.1 Stellar evolution theory

The basic theory of stellar interiors is one of the eldest in astronomy. Already Eddington (1926) was able to somehow model the at that time just discovered Hertzsprung-Russel diagram with the differential equations for stellar interiors. Currently all models are in principle based on his theory, although they have been improved and expanded to take into account our growing understanding of the physics of stars. For details about the current stellar evolution models, see e.g. the book of Salaris & Cassisi (2006) on the Evolution of Stars and Stellar Populations. Many ideas in this book are reflected in the website of the BaSTI models (<http://albione.oa-teramo.inaf.it/>), by the previous authors and others. One might wonder why there is such a large variety of stellar models presented on this website. The reason is obvious: the input physics is so uncertain that the final fit to the data will have to show what choices should be made. The stellar evolution model traces the evolution of stars of given mass and chemical composition through the various evolutionary phases defined from the color-magnitude diagrams of open and globular clusters, and provides the basic stellar parameters - bolometric luminosities, effective temperatures and surface gravities as a function of the evolutionary time. Apart from the BaSTI

models there are several other models available in the literature: e.g. the ones of Girardi et al. (2000), Marigo et al. (2008), Yi et al. (2003), Lejeune & Schaerer (2001), Dotter et al. (2007).

As far as the main stages of stellar evolution, it does not really matter very much which models one takes (see an earlier comparison study by Charlot, Worthey & Bressan 1996). What matters are the *later* evolutionary phases. For example, in the models of Vandenberg et al. (2000) no overshooting is used. The models do not go beyond the RGB, since the authors do not trust our understanding of the physics beyond that phase. It has to do with the treatment of convection and severe mass loss. The treatment of these phases (mainly the HB and the TP-AGB) varies considerably between groups. The BaSTI models, for example, give 2 sets of models for different mass loss rates η . For old stellar populations, for which the TP-AGB phase is unimportant, this means that this uncertainty plays a smaller role (see Mouhcine & Lançon 2002). In this paper it is shown that the fractional luminosity of the AGB in J , H and K is the highest between $\log(\text{age}) = 8.5$ and 9.2 , and reaches appr. 40% in J , 50% in H and 60% in K . The contribution also goes up with metallicity. In the future larger telescopes will provide us color-magnitude diagrams down to lower magnitudes, and the improved statistics obtained in this way will probably cause the stellar evolution calculations for these phases to considerably improve.

Another source of uncertainty is the He contents of stars (indicated as mass fraction Y). He comes mainly from Big Bang Nucleosynthesis, but it strongly affected by H and He-burning in stars. An important problem is that there are no easy ways to determine the He-content in stars. Atomic transitions generally require high-energy photons, so are mostly found in hot stars, and are found in the blue or difficult to access UV. Since He does affect the location of the stellar evolution tracks (see e.g. the BaSTI models) this is an important problem. More generally, recent models assume that the helium fraction is related to the metallicity Z (e.g. Vazdekis et al. (2010) use $Y = 0.23 + 2.25 Z$).

Not only is there a problem with He, there are more than 100 other elements that each can have their own relative abundance w.r.t. Fe. Traditionally, these are parameterized with Z , the mass fraction of all elements other than H and He. Luckily, the relative abundances of these *metals* do not vary very much. This is because it is thought that element production is a fairly uniform process: it is done mostly in supernovae, but also in the envelopes of giant or supergiant stars. However, one knows that different types of supernovae produce different relative fractions of elements: for example, since the rate of element production depends on stellar mass, the relative distribution of elements ejected into the ISM in a SN explosion must also depend on mass. Element ratios affect the stellar population models in 2 ways: both the evolutionary tracks change position (see e.g. the BaSTI models), but more importantly, their line strengths change more directly (see e.g. Lee et al. 2009). In section 1.3.4 this item will be discussed in more detail.

A third problem is the IMF (see before), which is very difficult to measure. This point will be discussed in section 1.3.3 and section 1.4.6.

Other problems occur when converting theoretical parameters (T_{eff} , g and

abundances) to observational ones, such as colors or spectra. These problems are enormous. Although it seems straightforward to determine temperatures from spectra of observed stars, this is difficult for M-stars, which have such broad absorption lines that complicated procedures are required to determine them (e.g. Lançon et al. 2008). For most stars reasonably accurate gravities are available from distances and CM-diagram fitting, and they will become better when the results of GAIA are available. Determining abundances of stars is a complicated subject, which is mostly done comparing line strengths of isolated transitions with stellar atmosphere models (e.g. MARCS (Gustafsson et al. 2008)). See e.g. Ryde et al. 2004 for a review. In the ideal situation these isolated transitions are available. However, in practise for many elements no lines are available. Often, the resolution of the spectra is so low that one a few elements can be investigated, or that less accurate methods will have to be used, such as only determining a global metallicity for galaxies. For hot stars, such as O or B stars, determining abundances is particularly difficult, since they contain almost no lines.

Apart from the models described above, the BaSTI website also provides models for pre main sequence stars and for white dwarfs. The role of contact binary stars is not considered. One way for them of manifesting themselves is through Blue Straggler Stars (BSS), hydrogen-burning stars made hotter and more luminous by accretion and now residing in a region of the color-magnitude diagram normally occupied by much younger stars (e.g. Bond & MacConnell 1971). The fact that they have been found in globular clusters (Piotto et al. 2004) shows that their presence can be significant in galaxies. Recently, such blue stragglers have also been detected in the Galactic Bulge (Clarkson et al. 2011). The reason that historically not much attention has been given to BSS in stellar population models is that in color-magnitude (CM) diagrams Blue Straggler Stars are not found in large quantities, and that integrated models of old ages do fit elliptical galaxies. Since ignoring Blue Stragglers would cause elliptical galaxies to appear younger, it is worthwhile to study this issue in the future.

1.3.2 Stellar libraries

An important ingredient in stellar population models is the *stellar library*. The stellar library is essential for the models. Its spectral resolution and wavelength range determine the spectral resolution and wavelength range of the models. Its range in stellar types determines the applicability of the models, and to a large extent their quality. It is defined as a set of spectra of stars, covering a range in stellar parameters, i.e. effective temperature T_{eff} , gravity g , and metallicity [Fe/H]. More recently, also abundance ratios, such as [Mg/Fe] are sometimes included (e.g. Milone et al. 2011). Stellar libraries can be theoretical (e.g. Hauschildt et al. (1997), Coelho et al. 2007) or empirical. Many of them can be found in the compilation of D. Montes (<http://www.ucm.es/info/Astrof/invest/actividad/spectra.html>). A good, but somewhat outdated review about empirical and theoretical stellar libraries is

given by Coelho (2009). As mentioned in the section above, SSP model spectra are determined integrating the spectral contributions from stars along isochrones, and weighting them with the relative fraction of stars at every place along those isochrones. The required spectra here are obtained by selecting the star (or linear combination of a few stars) with the required temperature, gravity and metallicity. This is generally done using some kind of interpolation.

The first often used stellar library was the LICK-IDS library (Faber et al. 1985, Burstein et al. 1984, Gorgas et al. 1993, Worthey et al. 1994). This library consists of 425 spectra obtained with a non-linear Image Dissector Scanner, which each had been reduced to 25 low resolution line indices defined as equivalent widths of strong absorption lines in the spectrum. For large galaxies, for which the velocity dispersions are so large that many faint features in the spectrum are washed out, a considerable amount of information between 4200 and 6400 Å is contained in these indices. This library since then has been by far the most popular stellar library, and has been used many times to derive stellar population parameters of galaxies. Since the library is quite noisy, special *fitting functions* were made for every index, to facilitate the interpolation in the library when calculating SSP models (see e.g. Worthey et al. 1994).

With the advent of linear CCDs soon more accurate stellar libraries became available, e.g. the library of Jones et al. (1997), which contains spectra, not just indices, covering 2 small wavelength regions. This library was used by Vazdekis (1999), who created the first stellar population models producing continuous output spectra. Now, 13 years later, among the most-used stellar libraries are MILES (Sánchez-Blázquez et al. 2006) and Elodie (Prugniel et al. 2007), although many other libraries exist, especially in the optical. The coverage of these libraries in terms of T_{eff} and $\log g$ is very good around solar metallicities. Outside the solar metallicity regime, the range of stellar population ages that can be modeled is somewhat restricted. The main problem at the moment is, that the wavelength range of these models is limited (e.g. the wavelength coverage of MILES is 3500-7500Å), and that only Galactic stars are included, most of them in the Galactic disk, implying that their abundance ratios reflect the formation history of the Galactic disk, with abundance ratios around solar. Recently, the MILES, CaT (Cenarro et al. 2003) and INDO-US libraries (Valdes et al. 2004) have been merged into the MIUSCAT library (Vazdekis et al. 2012), homogenizing resolution and flux calibrating, extending the library to 9500Å. The resolution of the current libraries goes from $R = \Delta\lambda/\lambda = 40000$ (Elodie) to about 2.5Å (MILES). A higher resolution, but still unpublished library is the UVES-POS stellar library (see Bagnolo et al. 2003), which has a resolution of 80000, but is not flux calibrated.

In the near-UV and the NIR, spectral libraries are smaller, with smaller ranges in stellar parameter space, but the situation is rapidly improving. In the near-UV the best library is (and will remain for some time) NGS, the Next Generation Spectral Library of Gregg, Silva and collaborators, containing spectra of 382 stars taken with HST/STIS at a wavelength-dependent resolution of 2000-10000, covering 1670–10250 Å with excellent flux calibration. In the NIR, a stellar library of 230 stars, the IRTF spectral library has recently become

available: a compilation of stellar spectra that cover the wavelength range from 0.8 to 2.5 μm at a resolution of $\sim 7\text{\AA}$ and for some from 0.8 to 5.0 μm (Rayner et al. 2009; Cushing et al. 2005). The library, which has been flux calibrated using 2MASS photometry mainly consists of late-type stars (F-M), AGB, carbon and S stars, and L and T dwarfs. Most of the stars are of solar-metallicity. Apart from this there is the stellar spectra of cool giants (Lançon & Wood (2000), which contains ~ 100 stars taken at a resolution of $R = 1100$.

Theoretical stellar spectra are reasonably reliable for stars down to G-type, since in later types molecular bands, which are still hard to model, are starting to dominate the spectrum. Colors in the visible and near-IR bands are reproduced within the error bars for temperatures down to 3500K. At a resolution of $R = 10^5$, the spectrum of the Sun is today reproduced to 5% of its relative flux, Arcturus (K1.5III) is reproduced to 9% and Vega (A0V) is reproduced to 1%. Residuals are in general larger towards cooler stars or lower surface gravities. For stars below 3500K, current developments in hydrodynamical models and pulsating atmospheres should improve the accuracy of the models, but it may well take some years before such grids are available to the completeness needed for population synthesis. For O- and B-type stars, recent developments in mass loss modeling, expanding atmospheres and wind features are being incorporated into the theoretical grids to model the UV with better accuracy (see Coelho 2009). Theoretical (or possibly semi-theoretical) libraries are the most promising to model the integrated spectral features of galaxies. As our understanding of stellar spectra improves, more and more analysis will be done with theoretical stellar libraries, especially in the optical and the near-UV. In the near-IR, I expect empirical libraries to remain highly superior for years to come. Progress should come from libraries with at the same time high spectral resolution and large wavelength coverage, such as the future X-Shooter spectral library XSL (Chen et al. 2011). By analyzing galaxies using at the same time optical, UV and near-IR features one should be able to constrain the old population dominating the mass, as well as recent or intermediate bursts of star formation at the same time.

1.3.3 The Initial Mass Function

An important ingredient in stellar population models is the Initial Mass Function. The IMF ultimately determines the mass to light ratio of a stellar population, and therefore choosing the right IMF is important to determine, among other things, the amount of dark matter in a galaxy.

Generally the IMF is determined by determining the *mass function* of stars and correcting them for their evolution, to establish the distribution of stars of a stellar population at birth. This can be done for stars in the solar neighborhood, or in Galactic clusters. A huge research effort has been invested to determine the shape and variability of the IMF. Many details about this can be found in e.g. the review by Kroupa (2007). Salpeter (1955) first described the IMF as a power-law, $dN = c m^{-\alpha} dm$, where dN is the number of stars in the mass interval $m, m + dm$ and c is the normalization constant. By modelling the spatial

distribution of the then observed stars with assumptions on the star-formation rate, Galactic-disk structure and stellar evolution time-scales, Salpeter determined α to be 2.35 for $0.4 < m < 10 M_{\odot}$. Later on, many other studies have extended the mass ranges to higher and lower mass stars. The current situation is that the stellar IMF *appears to be extra-ordinarily universal*, with an IMF which still has more or less the same slope down to about $0.5 M_{\odot}$, but turning over towards lower masses (the Universal IMF of Kroupa, his equation (20), see Fig. 1.4). Without such a turnover, the amount of mass in a stellar population can become very large, which often gets into conflict with dynamical measurements of mass in galaxies, since those should be at least as large as the mass in stars and stellar remnants. Kroupa also argues that the evidence for a top-heavy IMF is not strong in well-resolved starburst clusters, and that dynamical evolution of the clusters needs to be modelled in detail to understand possibly deviant observed IMFs. For the low-mass end of the IMF one has a reasonable idea of the IMF-slope down to about $0.2 M_{\odot}$ from star counts in the solar neighborhood. Also, here, the evidence for variations in the IMF is weak, although there might be some speculative systematic variation with metallicity in the sense that the more metal-poor and older populations may have flatter MFs as expected from simple Jeans-mass arguments. Bastian et al. (2010) in a review for Annual Reviews in Astronomy and Astrophysics confirms Kroupa's ideas: *We do not find overwhelming evidence for large systematic variations in the IMF as a function of the initial conditions of star formation. We believe most reports of non-standard/varying IMFs have other plausible explanations.*

In Section 1.4.6 we will look at evidence for different types of IMFs based on integrated stellar populations. This evidence should be considered in the light of the above mentioned detailed work in our Galaxy.

1.3.4 Abundance ratios

Abundance ratios of elements in galaxies contain a wealth of information about the way the stars were formed, and their formation timescales. Element production for elements heavier than He is thought to take place in stars. Explosions of supernovae and stellar mass loss cause these newly formed atoms to enter the interstellar medium, where they can be used to form new stars, which in turn can again enrich the interstellar medium later. It is thought that Supernovae type II (massive stars) and Ia (C-degenerate white dwarfs) are responsible for most of the matter ejected into the ISM. SN type II eject mostly so-called α -elements into the ISM (see Fig. 1.5), i.e. O, Ne and Mg. SN type Ia, which take longer to produce, since the stars first have to evolve to their white dwarf phase, mainly produce Fe-peak elements. The fact that the timescale of element production in these supernovae is so different makes it possible to use the abundance ratio of an α -element and a Fe-peak element as a star formation *clock*. A galaxy which forms all its stars early-on will have a much higher α /Fe ratio than a galaxy that forms its stars slowly.

In our Galaxy it has been possible to measure abundances of many elements since almost 20 years (Edvardsson et al. 1993). This paper shows that the

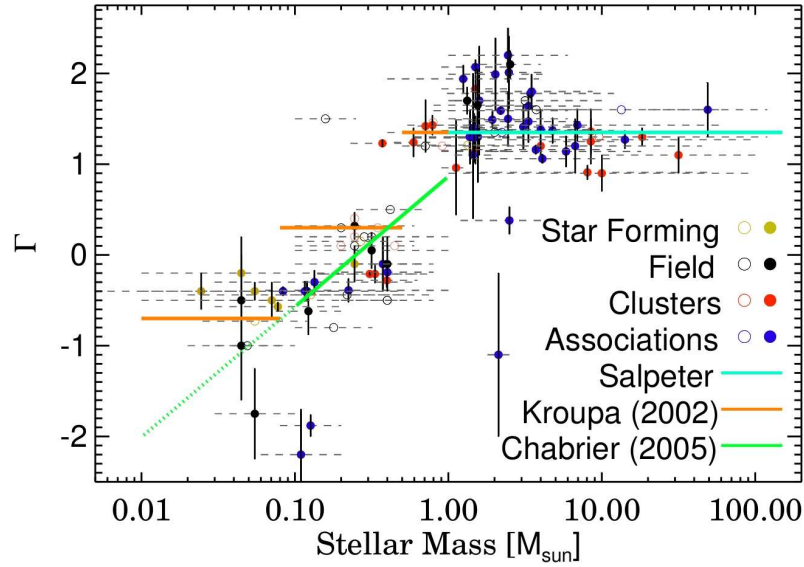


Figure 1.4: Derivative of the IMF-slope (Γ) as a function of stellar mass, derived from individual star counts (from Bastian et al. 2010). The colored solid lines represent three analytical IMFs: the Chabrier (2003) IMF (green), Salpeter (1955) in blue, and Kroupa (2001) IMF in orange.

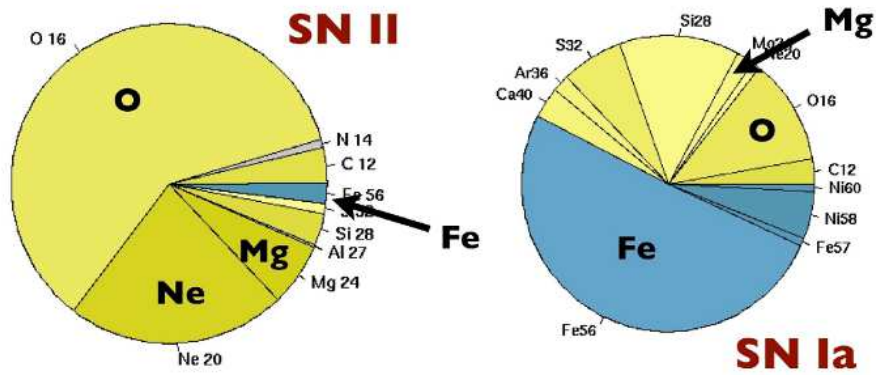


Figure 1.5: Supernova yields (= relative mass of metals released into the ISM at the death of the star), for SN type Ia and II. From Russell Smith, private communication.

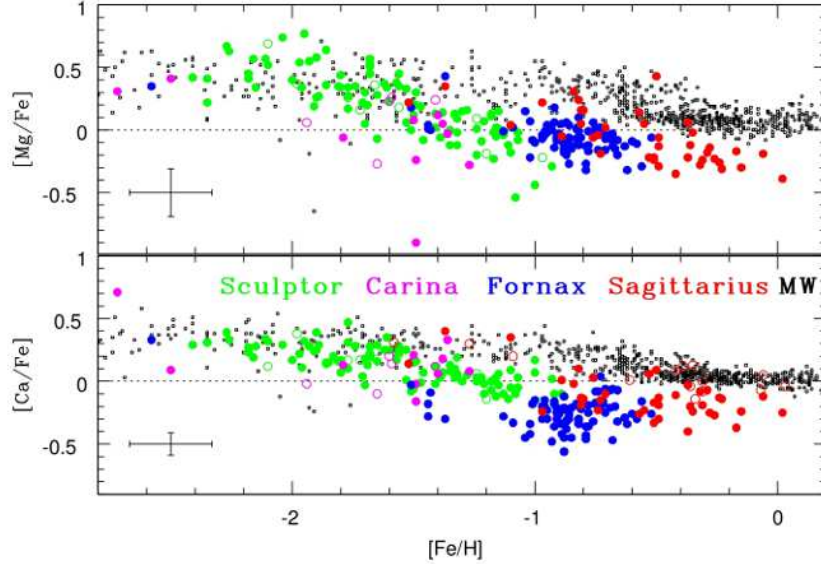


Figure 1.6: Abundance ratios of Mg/Fe and Ca/Fe for the Milky Way and a few local group dwarfs (from Tolstoy et al. 2009). For the origin of the individual measurements see Tolstoy et al. 2009.

[Mg/Fe] ratio for disk stars is higher than solar for low metallicity stars, and at a certain metallicity starts to flatten off towards the solar value. This means that when our Galaxy was formed, and the metallicity of stars was low, they formed quickly. After a number of generations of metal enrichment, star formation became slower, and element production by SN type Ia started taking over. A nice review about abundances and abundance ratios in our Galaxy and in the Local Group is given by Tolstoy et al. (2009). In Fig. 1.6 the current status of Mg/Fe measurements in the Local Group is shown. Dwarf galaxies each have their own *knee* in the [Mg/Fe] vs. [Fe/H] diagram, indicating the start of SN Ia element formation. The position of the knee indicates the metal-enrichment achieved by a system at the time SN Ia start to contribute to the chemical evolution (e.g., Arimoto & Yoshii 1987, and modelled by e.g. Matteucci & Brocato, 1990). This is between 10^8 and 10^9 yr after the first star formation episode. A galaxy that efficiently produces and retains metals over this time frame will reach a higher metallicity by the time SN Ia start to contribute than a galaxy with a low star formation rate.

Tolstoy et al. also explain that differences in relative abundances are to be expected between various α -elements. Conditions related to SN II explosions are responsible for the fact that O and Mg often show different trends with [Fe/H] than Si, Ca and Ti (e.g., Fulbright, McWilliam & Rich, 2007). Apart

from elements ejected into the ISM by SNe, also giant and supergiant stars are responsible for the enrichment of the ISM. For these evolved stars (giants or super-giants) material synthesized in the core will have been mixed to the surface layers, and ejected into the ISM through e.g. dust. Most of the material ejected in this way is C, N and O.

The production of heavy neutron capture elements is less well understood. One distinguishes 2 processes, depending on the rate at which these captures occur, and are called the slow (s-) and the rapid (r-) process. The s-process occurs in low to intermediate-mass thermally pulsating AGB stars (see Travaglio et al., 2004, and references therein). R-process production is associated with massive star nucleosynthesis. More about these elements and possibilities about using their abundances as star formation clocks can be found in Tolstoy et al.

I will discuss abundance ratios from unresolved galaxies in Section 1.4.3.

1.4 Stellar population analysis of individual galaxies

Having described the ways that stellar population models are being made, with some caveats about their capabilities, I will give some examples of their use in this section, indicating a number of issues that one has to be aware of when applying them. I will first discuss stellar population analysis on colors, and then on line indices or continuous spectra.

1.4.1 The age-metallicity degeneracy and luminosity weighting

Determining both an age and a metallicity of a galaxy, or even of an SSP, is tougher than it seems. Galaxy colors become redder as the galaxy ages, since more stars move to the giant branch, and also for increasing metallicities, since the effective temperatures of most stars decrease because of increasing opacities in the stellar photosphere. Colors and many line strengths in the optical basically depend on the temperature of the main sequence turnoff. The effects of increasing the age can be compensated for many observables by decreasing the metallicity. Worthey (1994) estimated that a factor of 3 increase in metallicity corresponds to a factor of 2 in age when using optical colors as age indicators, the so-called 2/3 rule. Optical colours are notoriously degenerated (see Fig.1.7 in the red part of the diagram).

There are, however, ways to break the degeneracy. Younger stellar populations with higher metallicities have a bluer contribution from the main sequence turnoff, and a redder one from the RGB. By using an optical color, together with a color that has a much higher relative sensitivity to the turnoff stars the degeneracy can be broken. This would be the case using colors such as $UV - V$, or Balmer line indices such as $H\beta$ or $H\gamma$. Equivalently, a combination of an optical color or line index which is strongly sensitive to the contributions of very

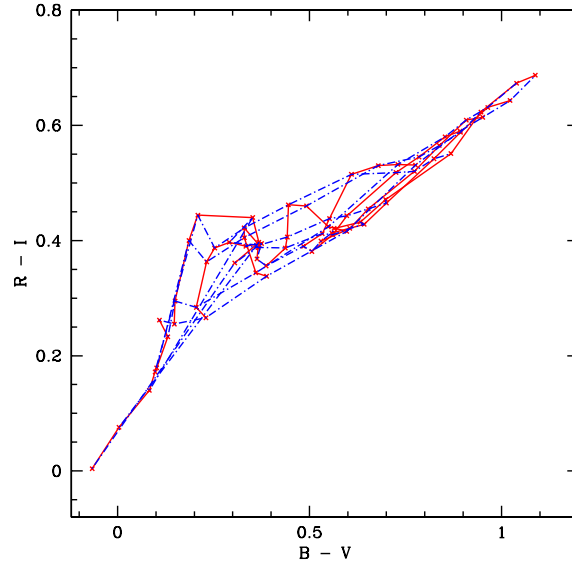


Figure 1.7: The age-metallicity degeneracy as seen in a color-color diagram. Shown is a grid of SSPs with varying metallicity and age. Especially in the right part of the diagram age and metallicity cannot be determined independently for given observations of $B - V$ and $R - I$. Used here are the MILES models (Vazdekis et al. 2010) with unimodal IMF and slope $x=1.3$.

cool giants would also break the degeneracy. Such colors would be e.g. $V - K$ or $J - K$, or the CO index at $2.3 \mu\text{m}$.

Both methods are being applied. For spectra covering only a small range in wavelength, very sophisticated indices have been developed maximizing age-sensitivity while minimizing the sensitivity to metallicity (e.g. Vazdekis & Arimoto 1999). In general, assuming that the stars in a galaxy are not coeval, a blue spectrum will give a different mean age than a red spectrum, since colors/indices in the blue will be more sensitive to the younger stars etc. This is the so-called *luminosity weighting* of stellar populations (I prefer not to use the term *light weighting*, since this has other associations, in e.g. material sciences). When applying stellar population synthesis codes, one should always realize that one's results have been weighted with the luminosity of the stars, implying that the brightest stars give the impression to be more important than they really are, when one weights according to mass, the natural choice. As an example, in the UV, sometimes 90% of the light in a cluster is coming from one star (Landsman et al. 1998) (see Fig. 1.8). This means that the mass-weighted age of that cluster could in principle be very old, while the luminosity weighted value is close the value for that star, i.e. young. For the interpretation of galaxy ages this

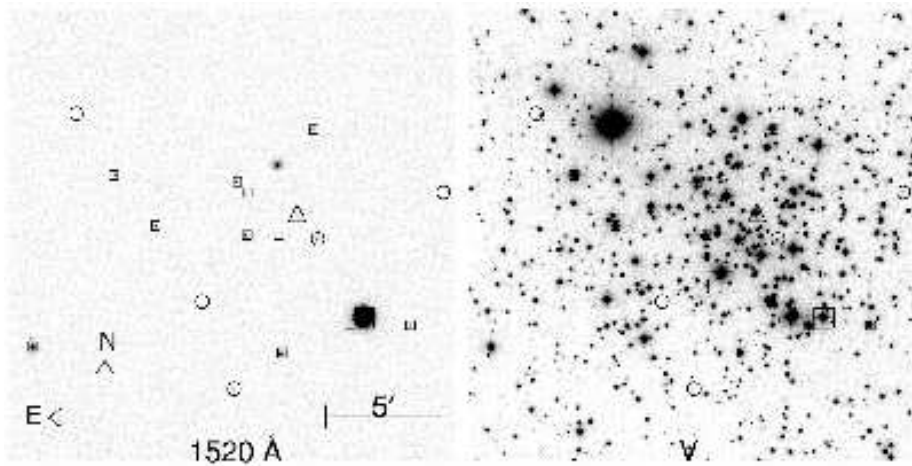


Figure 1.8: UIT image at $\sim 1500\text{\AA}$ and in V of the open cluster M67 (Landsman et al. 1998). Note that one star completely dominates the light in the UV.

distinction between mass and luminosity weighting is particularly important.

1.4.2 Analysis using colors, and the role of extinction

In Chapter 1.3 we have found out that stellar populations in globular clusters are SSPs, and that populations in galaxies can be considered as linear combinations of SSPs. Recently, however, we have learned that the first assumption does not always hold. For a while it has been known that ω Cen, which up to now was considered to be a globular cluster, shows a spread in metallicity and possibly also age (Norris & Da Costa 1995). Conservative people could maintain for another 10 years that globular clusters have a single metallicity, by claiming that ω Cen is a galaxy, until recently Piotto et al. (2007), see Fig.1.9, discovered multiple main sequences in the globular cluster NGC 2808. At the same time Mackey & Broby Nielsen found multiple main sequences in the LMC cluster NGC 1846. More clusters have been found later showing similar effects (e.g. Milone et al. 2008, Mackey et al. 2008). It is not clear yet what the reason is of these multiple branches. It could be that the He (or CNO) abundance is different, but also there might be a difference in age/metallicity. Spectroscopic studies here will have to show what really is happening.

Color-magnitude diagrams can not only be used for globular clusters but also for galaxies in the rest of the Local Group. With HST it is possible to resolve individual stars below the Main Sequence Turnoff, and this way obtain exquisite star formation histories. In Fig. 1.10 I have reproduced a figure from the review of Tolstoy et al. (2009) with star formation histories of 3 dwarfs. An earlier, also excellent review, is by Mateo (1998). The star formation histories show that there are large variations between the galaxies of the local group, even between

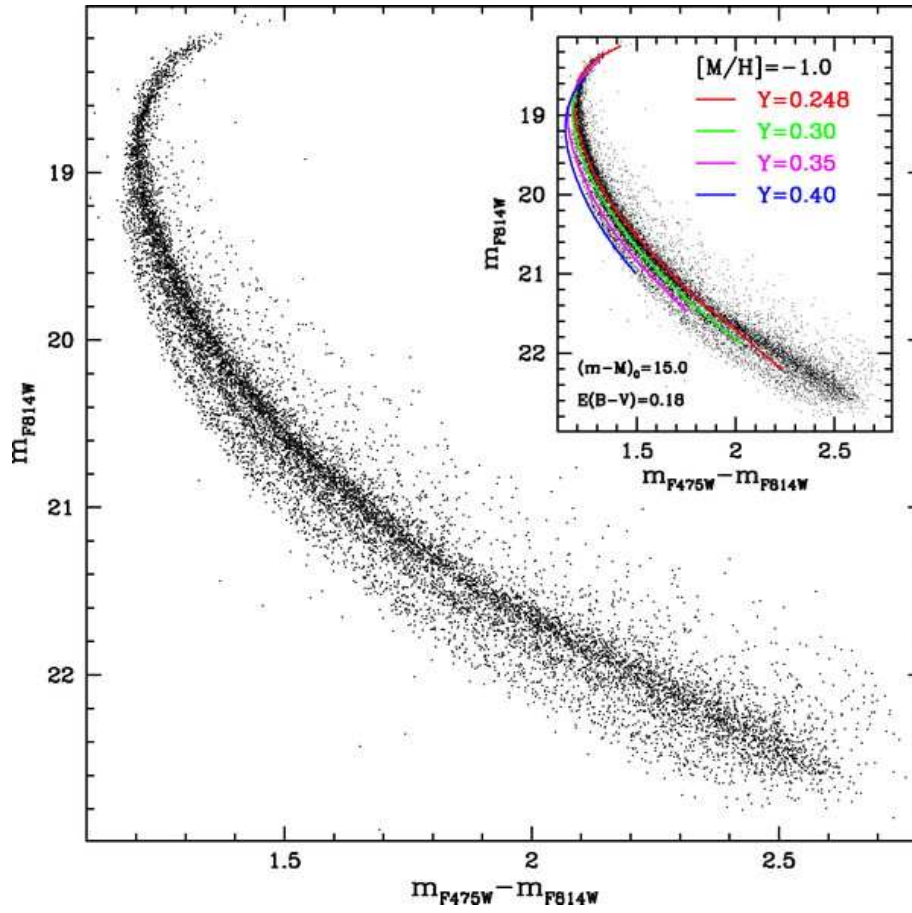


Figure 1.9: Differential reddening corrected CMD of the globular cluster NGC 2808. In the inset some fits have been done with models of age 12.5 Gyr and various He abundances (from Piotto et al. 2007).

galaxies that have the same morphological classification (M32, NGC 205 and NGC 185). There are no galaxies for which we can exclude the presence of an underlying old population. Radial gradients in the populations of individual galaxies are seen as well. As mentioned before, more information about the abundance ratios in individual stars, giving information about star formation timescales, can be obtained from spectroscopy of bright giants in these galaxies.

When one goes further away, one can only resolve stars on the Red Giant Branch and beyond. One can obtain the spread in metallicity, e.g. in Centaurus A (Harris et al. 1999), and the galaxies in the ANGST survey (Dalcanton et al. 2009). A great application of counting the stars on the RGB is to use these star counts to make maps of the stellar density in the outer parts of galaxies. This way people have found huge low surface brightness features linking M31 with its companions, including M33, probably remains from encounters between these galaxies (Ibata et al. 2001, McConnachie et al. 2009). For the spiral galaxy NGC 300 Bland-Hawthorn et al. (2005) have been able to measure the stellar surface brightness profile to a distance of 10 effective radii from the galaxy center in this way.

In Fig. 1.11 a closeup is given of an RGB image of the disk of NGC 891, a nearby edge-on galaxy. What is clear are the many bright stars in the disk of the galaxy. Above it, many red filaments are seen. They are dust-lanes, seen up to large distances from the plane. In the lectures by Daniela Calzetti (this volume) you can see a lot of material about this dust, and how it extinguishes the light behind it. In Fig. 1.11 for example, further study shows that the blue stars seen in the left bottom corner are found in front of most of the disk of the galaxy, which itself is barely seen because of the extinction. In Fig. 1.12 one can see that the extinction is usually associated to spiral arms, and that it can be present to large radii. Here the extinction in a spiral disk is seen in front of an elliptical galaxy.

Dust extinction is found predominantly in spiral galaxies of type Sab-Sc (e.g. Giovanelli et al. 1994). It is generally associated to molecular gas, and is stronger in larger (higher metallicity) galaxies. The UV energy absorbed by the dust is re-radiated in the IR and submm, responsible for a large fraction of the emission at those wavelengths. As far as stellar population synthesis is concerned the most important effect is that it reddens the colors using the dust extinction law (e.g. Cardelli et al. 1989). Reddening is strongest in the blue, and almost non-existent red-ward of $2 \mu\text{m}$. In our Galaxy, it is impossible to see the Galactic Center in the optical, because of more than 20 magnitudes of extinction. However, in the infrared, at 2 micron, the extinction is only about 2 mag, so that observations there are easily possible. The ratio of reddening of dust in various colors is very similar to the effect of metallicity (and even age). This means that by simply measuring two colors, one cannot correct for the effects of extinction. For that more colors, or a spectrum are needed. It is therefore also not easy to measure the extinction from colors in a spiral galaxy. If one wants to do this, one can e.g. measure the amount of extinction statistically, by looking at the dependence on inclination. The color of a galaxy without extinction should not depend on inclination, while for an inclined galaxy

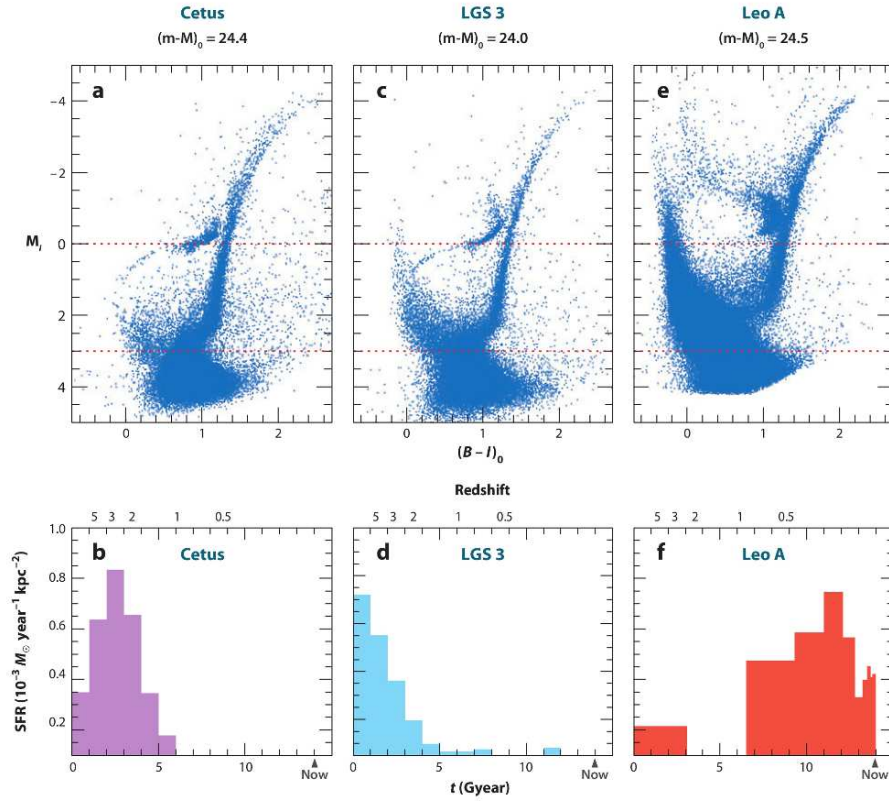


Figure 1.10: HST/ACS color-magnitude diagrams SFHs for three Local Group dwarf galaxies: Cetus, a distant dwarf spheroidal galaxy LGS 3, a transition-type dwarf galaxy and Leo A, a dwarf irregular. These results come from the LCID project (Gallart & the LCID team 2007, Cole et al. 2007). From Tolstoy et al. (2009).

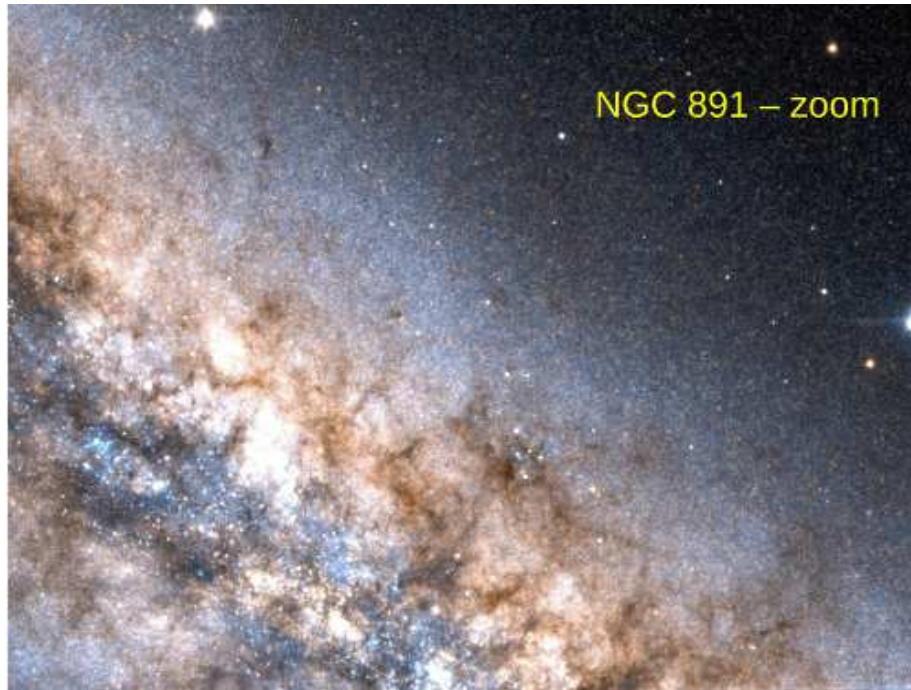


Figure 1.11: Composite HST F814W/F555W image of NGC 891 (from the Hubble Legacy Archive). This galaxy is sometimes called the *twin* of our Milky Way. Note the young stars in the mid-plane and the dust extinction filaments.

the path length through the dust is longer, and thus the extinction. In Peletier et al. (1995) this technique is used to show that many nearby spiral galaxies in the B -band are optically thick within their central effective radius, but not in their outer parts. Certainly in bulges extinction plays a large role in many galaxies, and people analyzing the colors of external bulges should take this into account (e.g. Balcells & Peletier 1994).

In the absence of dust color-color diagrams consisting of an optical and an optical-IR (or IR) color, or, e.g., of a UV-Opt and an optical color, can be used to separate the effects of age and metallicity. This method is popular for globular clusters in nearby galaxies, for which high quality spectra are difficult to get. As can be seen in Fig. 1.13, it is important that accurate observational colors are available. Such studies can maybe explain the bi-modality in globular cluster colors (Ashman & Zepf 1992). Chies-Santos et al. (2012), for a sample of 14 early-type galaxies, found that, although the optical color distributions of the globular clusters are bimodal, this is not always the case in the infrared (z -K). The authors explain this results with a non-linear color-metallicity conversion, but clearly state that better data are required to confirm their results.

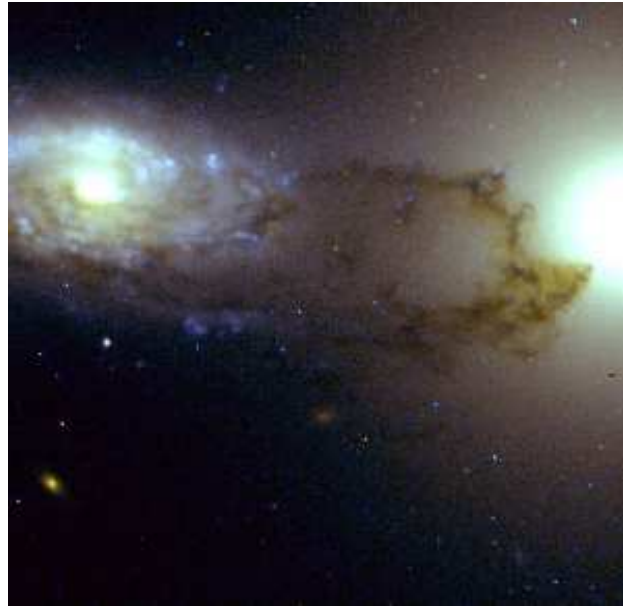


Figure 1.12: Dust in a spiral galaxy seen in absorption in front of an elliptical galaxy (from White & Keel 1992).

This means that colors of globular clusters are not well understood. The, up to recently, firm conclusion that globular clusters have a bimodal metallicity distribution is now up for discussion.

The same color combination is also often used for galaxy research. In Fig. 1.13 (right) HST data are shown of the inner parts of a sample of early-type spiral galaxies (Peletier et al. 1999), on top of a grid of SSP models. Central colors are indicated with red, filled symbols, while the colors at 0.5 bulge effective radii are indicated in open, blue circles. These latter colors are calculated on the minor axis of the bulge, on the side not obscured by the galaxy disk. Interesting to see from this plot is that most galaxy centers lie, often far, away from the model grid, indicating considerable amounts of extinction A_V of often more than 1 magnitude. The blue points cluster mostly together. Although the exact position of the model grid should be taken with caution (color differences are probably more reliable than exact colors, because of systematic effects in the models), this diagram seems to indicate that the bulges in this sample are old (mostly around 8-9 Gyr) with metallicities somewhat below solar.

The fact that one has to determine such detailed colors leads to another problem: the models. Up to recently, the spectrophotometric quality of the stellar population models has not been very high. In Sánchez-Blázquez et al. (2006) it is shown that the colors of stars in the MILES sample are consistent with their spectra within 1.5%, something which cannot be said from e.g. the

Stelib library (Le Borgne et al. 2003), used for the Bruzual & Charlot (2003) models. Vazdekis and his group have extended the MILES library with a subset of good spectra from the Indo-US library (Valdes et al. 2004), with the aim of making a stellar library with wavelengths up to 9500Å with good flux calibration. In Ricciardelli et al. (2012) they show that, when fitting well-calibrated SDSS data, there are problems fitting the $g-r$ vs. $r-i$ distribution of galaxies for galaxies with high velocity dispersions. In this paper it is discussed that probably α -enhanced stellar population models are needed to solve this issue.

1.4.3 Analysis using optical spectra

The main difference between a spectrum of a star and one of a composite system, such as a galaxy, is that the composite spectrum is the sum of many stellar spectra, weighted by their flux at the particular wavelength, and shifted by their individual radial velocities. These velocity shifts are not to be discarded. In a large galaxy stars move through one another with a velocity dispersion of about 300 km/s. This means that every line in the spectrum is broadened by a Gaussian with such a dispersion, which means that abundances can not be measured any more from narrow lines from single transitions, since those are all blended. Abundances have to be obtained by fitting stellar population models with given abundances to the galaxy spectra. Velocity broadening cannot be avoided, and we have to live with broadened lines. The most common way to measure line strengths in composite spectra is by using a system of line indices. These indices are defined by three pass-bands: a feature band, and two continuum bands, and measured as equivalent width: the surface (in Å) under the spectrum that is normalized using the continuum on both sides (see Worthey et al. 1994 for definitions of the Lick/IDS system. In the Lick/IDS system 21 indices were defined to measure the strongest stellar features in the spectrum in the optical at a resolution of about 9Å (Worthey et al. 1994). 4 more indices (2 H γ and 2 H δ indices) were added in 1997 by Worthey & Ottaviani. These indices were used by Trager et al. (2000) to determine stellar population parameters from Lick/IDS indices of many nearby galaxies. Later-on, many more indices were added by Serven et al. (2005). Other indices are available in the literature. Rose (1994) defined several indices with a one-sided continuum, mainly in the blue. Cenarro et al. (2001) defined indices in the region of the Ca II IR triplet, sometimes with with multiple continuum regions. Normally an index becomes larger as the absorption line becomes stronger. Some lines, however, like the H δ and H γ lines in the Lick system, are situated in such crowded regions, that their continuum fluxes are affected by metal abundances, and that the line index sometimes can be negative, even though H γ or H δ is found in absorption.

Lick indices are hard to measure. Not only do they require the observed (galaxy) spectrum to be convolved to exactly the right resolution, and do they require a rather uncertain correction for velocity broadening, they also need certain zero point corrections to make sure that the instrumental response of the observed spectrum has the same shape as the Lick/IDS in the 1980's, when the standard stars for the Lick system were observed. This is a tedious job, since

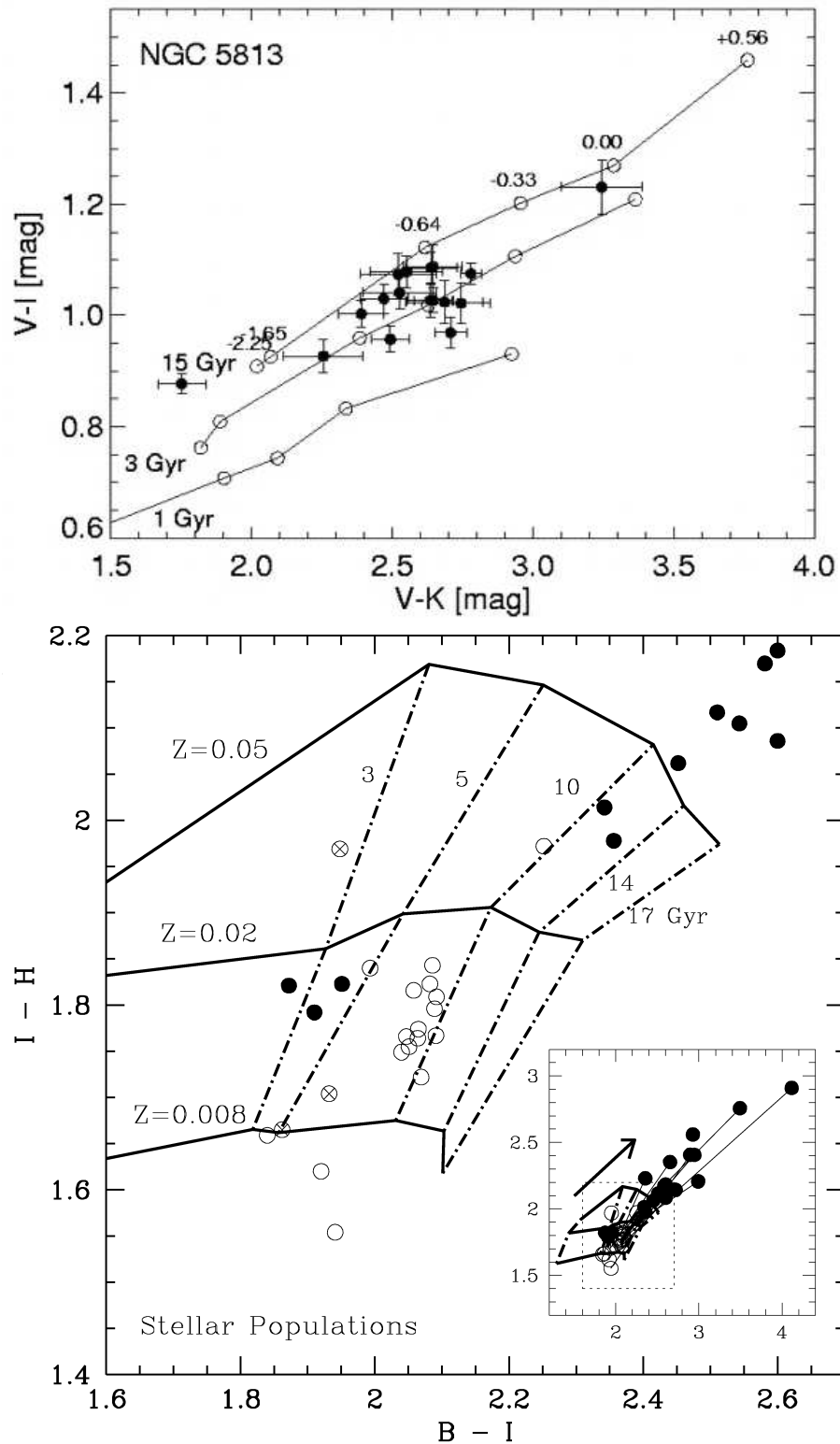


Figure 1.13: Top: $V-I$ vs. $V-K$ diagram for globular clusters in NGC 5813 (from Hempel et al. 2007). Bottom: $B-I$ vs. $I-H$ diagram for bulges of early-type spirals (from Peletier et al. 1999).

the Lick system does not work with flux calibrated spectra, and requires that for every observational setup a number of Lick standards are observed. To improve the situation, a slightly modified line index system (LIS) has been defined by Vazdekis et al. (2010). It is based on the MILES stellar library, uses the same wavelength definitions as the Lick/IDS system, and is defined on flux calibrated spectra, so that it is much easier for people to use this backward compatible system. To make it possible to also use less broad indices, for e.g. globular clusters and dwarf galaxies, the LIS system has been defined for standard resolutions of 5, 8.4 and 14 Å FWHM.

Although line indices are a good way to measure the strength of certain spectral features, there is, at present, no need any more to go through the indices, when comparing galaxy data with models, since one can directly fit the models to the data. Vazdekis (1999) already showed the power of this method, which dramatically can show regions of the spectrum where the models are inadequate (see Fig.1.14). Of course, the stellar population models will have to be convolved with the correct LOSVD (Line of Sight Velocity Distribution), i.e. the broadening of the stars. The SAURON team (Sarzi et al. 2006) have applied full spectral fitting to Integral Field Spectroscopy of ellipticals and S0s, fitting the observed spectrum at every position in every galaxy with a set of SSP models, determining the LOSVD, and a best-fit stellar population model. They noticed that always large residuals occurred at the position of emission lines such as $H\beta$ and the [OIII] line at 5007Å. Realizing that they could at the same time also measure the velocity and broadening of the ionized gas, they then developed a method to fit at the same time velocity broadened SSP models and Gaussians representing the emission lines to the data. As a result, ionized gas could be found in 75% of the sample, much more than was previously known. This method is much more sensitive than e.g. methods that map emission lines using narrow-band filters. Of course, those latter methods can cover a larger area, at generally a higher spatial resolution.

Separating absorption and emission is in particular important for lines which are at the same time important absorption and emission lines, such as the Balmer lines $H\beta$ and $H\gamma$. These lines, which are so important to determine ages of stellar populations, can easily be filled in by emission. Before full spectral fitting was possible assumptions were made that the $H\beta$ emission line strength was a constant fraction of the [OIII] 5007Å line. The maps of Sarzi et al. (2006, 2010) show, however, that this ratio varies from galaxy to galaxy. Methods like this are so powerful that Balmer absorption line strengths can be measured in spiral galaxies with strong emission lines (e.g. Falcón-Barroso et al. 2006, MacArthur et al. 2009).

The most popular index-index diagram is the Mg b vs. $H\beta$ diagram. Here Mg b is mostly sensitive to metallicity, while $H\beta$ is mostly age-sensitive. Using this diagram it was found that massive galaxies have α /Fe ratios higher than solar (Peletier 1989, Worthey et al. 1992). In Fig. 1.15 we show $H\beta$ against [MgFe50], a composite of the Lick indices Mg b and Fe 5015, from Kuntschner (2010). Here one sees how some relatively small differences between stellar population models can change the ages derived from these indices. Here the

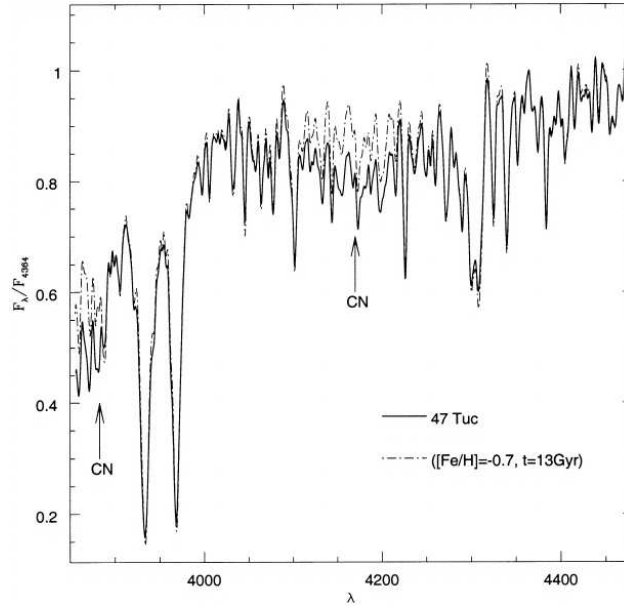


Figure 1.14: Blue spectrum of 47 Tuc, together with an SSP fit by Vazdekis (1999). Marked are the well-known CN strong bands of this globular cluster.

models of Schiavon (2007) and those of Thomas et al. (2003) are shown. The galaxies are from the SAURON sample of early-type galaxies, and are shown as lines, with a dot in the center. Using the models of Schiavon, the old galaxies (these are mostly the ellipticals and the massive S0's) are old everywhere, with metallicity decreasing outwards. If one uses the models of Thomas et al. (2003), the outer parts are older, with similar metallicity gradients. Note here that these ages are luminosity weighted ages, and that the younger galaxies probably consist of an older continuum with a young population superimposed.

Measuring element abundance ratios from integrated spectra is much less straightforward than for individual stars. What we know is that $[Mg/Fe]$ varies strongly as a function of galaxy velocity dispersion σ (a proxy of mass). We also know that α -elements vary more as a function of σ than Fe (Sánchez-Blázquez et al. 2006). From a sample of galaxies in the Coma cluster Smith et al. (2009) and Graves & Schiavon (2008) claim that the abundance ratios Mg/Fe and Ca/Fe simultaneously decrease with Fe/H and increase with σ . These dependences can be explained by varying star formation time scales as a function of σ , and therefore different ratios of element enrichment by SN type II and Ia. For both C/Fe and N/Fe , no correlation with Fe/H is observed at fixed σ . This can be explained if these elements are produced primarily by low/intermediate mass stars, and hence on a similar time-scale to the Fe enrichment. The element abundance ratio trends with $[Fe/H]$ are very similar to those in our Galaxy,

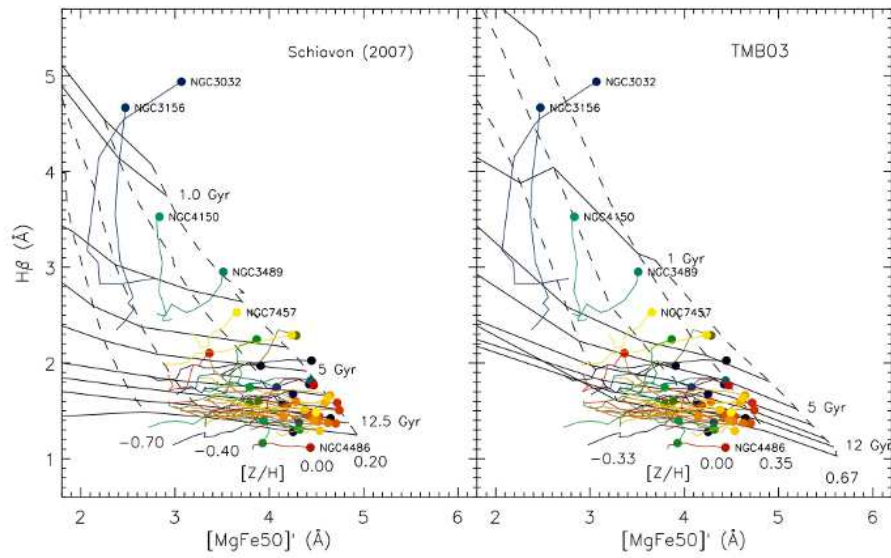


Figure 1.15: Radial line strength gradients for the 48 early-type galaxies in the SAURON sample. The center of each galaxy is indicated by a filled circle and different colors are used for each galaxy. Over plotted are stellar population models by Schiavon (2007, left) and Thomas et al. (2003, right) for solar abundance ratios. Note that the latter models extend to $[Z/H] = +0.67$, whereas Schiavon models reach only $[Z/H] = +0.2$ (from Kuntschner et al. 2010).

which suggests a high degree of regularity in the chemical enrichment history of galaxies (Smith et al. 2009).

1.4.4 Star Formation Histories and the SSP

The availability of full spectra makes it possible to recover the Star Formation History (SFH) in some detail. Here one can divide the efforts into 2 parts: efforts that fit the full spectrum, including UV and IR, using the far IR, originating mostly from dust emission, as well as the submm on one hand, and more detailed studies that determine the distribution of stars of various ages on the other. The most important result from the first kind of studies is the amount of hot, young stars, responsible for ionizing the gas and heating up the dust around them. For this work I refer to Daniela Calzetti's chapter in this book.

As far as the analysis of photospheric light is concerned, there is a growing body of full spectrum fitting algorithms that are being developed for constraining and recovering the Star Formation History (e.g., MOPED - Panter et al. 2003; Starlight - Cid Fernandes et al. 2005; Steckmap - Ocvirk et al. 2006; Koleva et al. 2008). SED fitting works best for large wavelength ranges. It is based on a set of SSP models and an extinction curve, and fits at the same time the stellar population mix, the LOSVD and the amount of extinction.

Using full spectrum fitting several independent bursts of star formation can be determined. The number of parameters that can be recovered from a spectrum depends strongly on the signal-to-noise ratio, wavelength coverage and presence or absence of a young population (Tojeiro et al. 2007). However, the results are strongly affected by the age-metallicity degeneracy, so interpreting the results is difficult. Also, there is a certain degeneracy between the number of components in the LOSVD, and the SFH. Some tests are shown in Ocvirk et al. (2008), who try to constrain at the same time the SFH and the LOSVD along the slit of the spiral galaxy NGC 4030. It is clear from this experiment that higher spectral resolution and S/N data is needed to obtain astrophysically reliable results which are not degenerate.

On the other hand, such studies are very useful to determine whether a galaxy is well fit by a one-SSP model, and if this is not the case, what the relative mass fraction in the various components in the SFH is. That information is useful to understand the formation history, combining it with spatial information about e.g. interactions. I will give 2 examples here.

The first is by Koleva et al. (2009). They derive star formation histories of dwarf ellipticals in the Fornax cluster using ESO-VLT data. To understand the formation of these galaxies, it is very important to know whether these star formation histories are extended or short-lived, and whether they are very diverse, as is the case in the Local Group. In the Fornax cluster the environment is different, with a stronger influence from the IGM. Usually the photometric images are featureless, so that little can be learned about the stellar populations from the morphological structure. The results show that the star formation histories are not very different from those in the Local Group, and vary from SSP-like to extended (Fig.1.16).

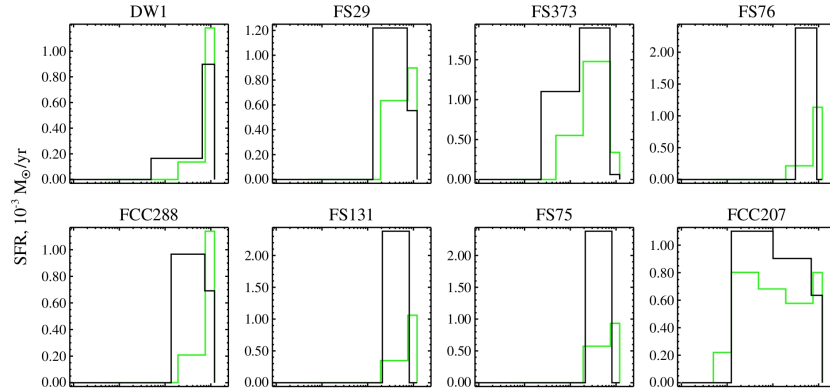


Figure 1.16: Star formation histories for the inner arcsec of a number of dwarf ellipticals, from Koleva et al. (2009). Black lines indicate SFR obtained using Steckmap, green using ULYSS.

A second example is from MacArthur et al. (2009), who determined star formation histories in a sample of late-type spirals using long-slit high S/N Gemini/GMOS data. For these spirals, imaging already shows that they have composite stellar populations. This is confirmed and quantified by stellar population synthesis. The authors are able to derive star formation histories consisting of a number of logarithmically spaced SSPs. One of their most important conclusions is that, although young populations contribute a large fraction to the galaxy light of late-type bulges, in mass they are predominantly composed of old and metal rich SPs (at least a mass fraction of 80%).

1.4.5 Learning about stellar populations using 2D spectroscopy

In the previous sections we have discussed how to derive the star formation history of a stellar population at a given position in a galaxy. One should always remember that galaxies are morphological and dynamical entities, and that the stellar populations that one derives are the result of the formation and evolution of the galaxy, and therefore intimately related to the morphological/kinematical component that one studies. 2-dimensional spectroscopy is an ideal tool to connect stellar populations with morphology and dynamics. In the last decade many of the large galaxies in the nearby Universe have been studied using the SAURON instrument at La Palma. The NIR Integral Field Spectrograph Sinfoni at ESO's VLT is making a large impact in the field at galaxy formation at $z \sim 2$ (SINS survey - Förster-Schreiber et al. 2009). Many IFU surveys are being planned (e.g. CALIFA, Sánchez et al. 2012; VIRUS, etc.).

The SAURON survey (de Zeeuw et al. 2002, Bacon et al. 2001) has shown

that many early-type galaxies contain kinematically-defined central disks. $H\beta$ absorption maps often show that these disks contain stars that are younger than the stars in the main body of the galaxy. The connection here between the stellar populations, the morphology and the kinematics shows us that these disks are formed later. Since most of the disks have angular momentum that has the same sign as that of the main galaxy, one thinks that the disks are formed from gas lost by stars in the galaxies themselves (Sarzi et al. 2006). Spiral galaxies, much more than elliptical galaxies, have several components, such as bulge, inner disk, outer disk, bars, rings, etc. Here studying the stellar populations together with morphology and dynamics much more enhances our understanding of all these components, and the galaxies as a whole. I will discuss here the inner regions of 2 spiral galaxies, in order of morphological type, from the SAURON study of Falc3n-Barroso et al. (2006) and Peletier et al. (2007).

The first one is the Sa galaxy NGC 3623 (Fig. 1.17). The inner regions of this galaxy mainly contain old stellar populations, as shown by the absorption line maps and confirmed by the unsharp masked HST image, an image which is a very good indicator of dust extinction. Since young stars are always accompanied by extinction, unsharp masked images are an efficient way to find younger stars. However, the presence of dust is not always sufficient to detect young stars. The radial velocity map shows an edge-on, rotating disk in the center, confirmed by a central drop in the velocity dispersion. This central disk contains old stellar populations, probably slightly more metal rich (see the age and metallicity maps).

The next galaxy is also an Sab galaxy, NGC 4274 (Fig. ??). This galaxy seems not to be very different from the one before. The unsharp masked image shows a central spiral, which might be similar to the one in NGC 3623 (which is edge-on, so the spiral structure in the dust cannot be seen). This spiral is associated to a rotating feature, seen both in the velocity and the velocity dispersion maps. In both galaxies, ionized gas is present everywhere in the central regions (Falc3n-Barroso et al. 2006). Different from NGC 3623, the stellar populations in the central disk in NGC 4274 are much younger than in the main body of the galaxy, as can be seen from the line strength maps, especially $H\beta$ absorption. If one now looks at the photometric decomposition (Peletier 2009), one sees that the part of the surface brightness profile of NGC 4274 that lies above the large exponential disk, i.e. the bulge, corresponds to the region of the inner disk, and is best fitted by a S3ersic profile with $n = 1.3$. In the case of NGC 3623 the so-defined bulge is much larger, and has a S3ersic index of $n = 3.4$. Kormendy & Kennicutt (2004) would call the bulge in NGC 4274 a pseudo-bulge, and the one in NGC 3623 a classical bulge. However, the comparison here shows that both objects are very similar, but that only the inner disk to elliptical bulge ratio in both galaxies is different. The study of other bulges in this sample shows that many early-type spiral galaxies contain central disks, with often young stellar populations in them.

The study of the central stellar populations and dust can also be done very well using IRAC on the Spitzer Space Telescope. van der Wolk (2011) in his PhD Thesis presents color maps of these SAURON-selected spirals. Information

about the ages of the stellar populations comes from the $[3.6] - [4.5]$ maps (see Section 1.5.2). In Fig.1.19 the $[3.6] - [8.0]$ maps of the 2 galaxies are shown. These maps show the amount of warm dust (mainly due to PAHs). One can see that in NGC 3623 relatively little warm dust is present, consistent with the absorption line maps, while much more is present in NGC 4274.

1.4.6 Stellar masses and the IMF in galaxies

Spectra and colors of SSPs are fairly insensitive to the initial mass function (IMF), because most of the light comes from stars in a narrow mass interval around the mass of stars at the main sequence turnoff. On one hand this is good, because it allows modelers to produce predictions for the spectra of galaxies that are accurate at most wavelengths. However, the same effect makes it possible to hide a large amount of mass in the form of low mass stars in a stellar population, making the stellar mass-to-light ratio a badly constrained parameter. Colors and lines of galaxies can generally be fitted well with a Salpeter IMF (a power law function with $x=1.3$, see above). However, the same observables can also be fitted with an IMF that flattens below a certain critical mass, e.g. the Chabrier (2003) IMF, which flattens off below $0.6 M_{\odot}$, giving a M/L ratio which is a factor 2 lower.

Until the end of the 1990's the uncertainties in the IMF were considered so important that estimates of stellar mass were rarely given. This changed with the influential paper by Bell & de Jong (2001), who showed that if one maximized the stellar mass in the disk when reproducing rotation curves of galaxies (the so-called maximum disk hypothesis) an IMF similar to the Salpeter IMF at the high-mass end with fewer low-mass stars, giving stellar M/L ratios 30% lower than the Salpeter value, was preferred. After this, it has become very common that stellar masses are given when fitting lines or colors of galaxies. In the important paper of Kauffmann et al. (2003), where stellar masses of many galaxies in the SDSS survey are calculated, the Kroupa (2001) IMF is used, a similar kind of IMF, and in only 2 sentences the authors mention that there can be systematic uncertainties in the derived stellar masses, as a result of the choice of the IMF.

Although in the optical most features are only slightly sensitive to the IMF-slope, there are some, mainly in the infrared, which strongly depend on the dwarf to giant ratio, i.e. the IMF-slope. Examples are the Wing-Ford band at $0.99 \mu\text{m}$, the Na I doublet at 8190 \AA , and the Ca II IR triplet around 8600 \AA . These lines have been used by several authors to constrain the IMF-slope (e.g., Spinrad & Taylor 1971, Faber & French 1980, Carter et al. 1986, Schiavon et al. 2000, Cenarro et al. 2003), but the results have never been very conclusive. The most important reason for this is that telluric absorption lines make it hard to measure accurate line strengths in this region of the spectrum. The second reason is that it is not always straightforward to derive the IMF-slope from the observations. For example, in Fig.1.4.6 Cenarro et al. showed, based on the strength of the Ca II IR triplet and a molecular TiO index, and on the anti-correlation between the strength of the Ca II IR triplet and the velocity dispersion, that the IMF

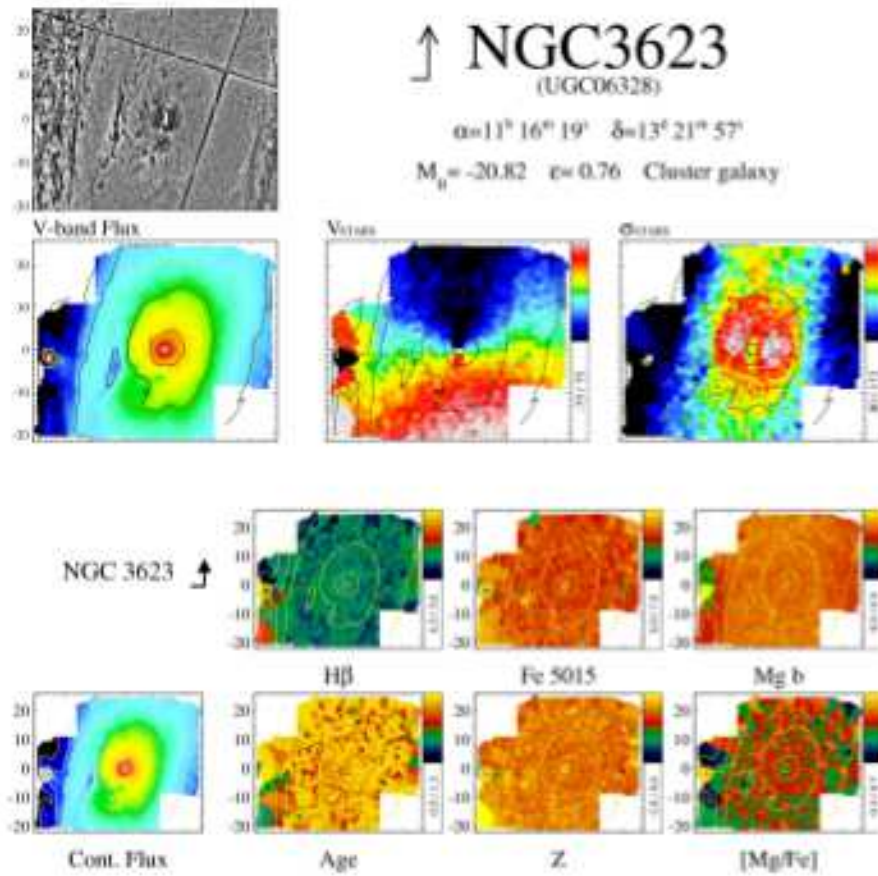


Figure 1.17: 2-dimensional maps of various quantities in the inner regions of NGC 3623: (from top left to bottom right): unsharp masked HST image, V-band continuum image, stellar velocity field and velocity dispersion maps, $H\beta$, Fe 5015 and Mg b absorption line maps, again V-band continuum image. age, metallicity and $[Mg/Fe]$ map. All from SAURON (Falc3n-Barroso et al. 2006, Peletier et al. 2007), except for the HST image.

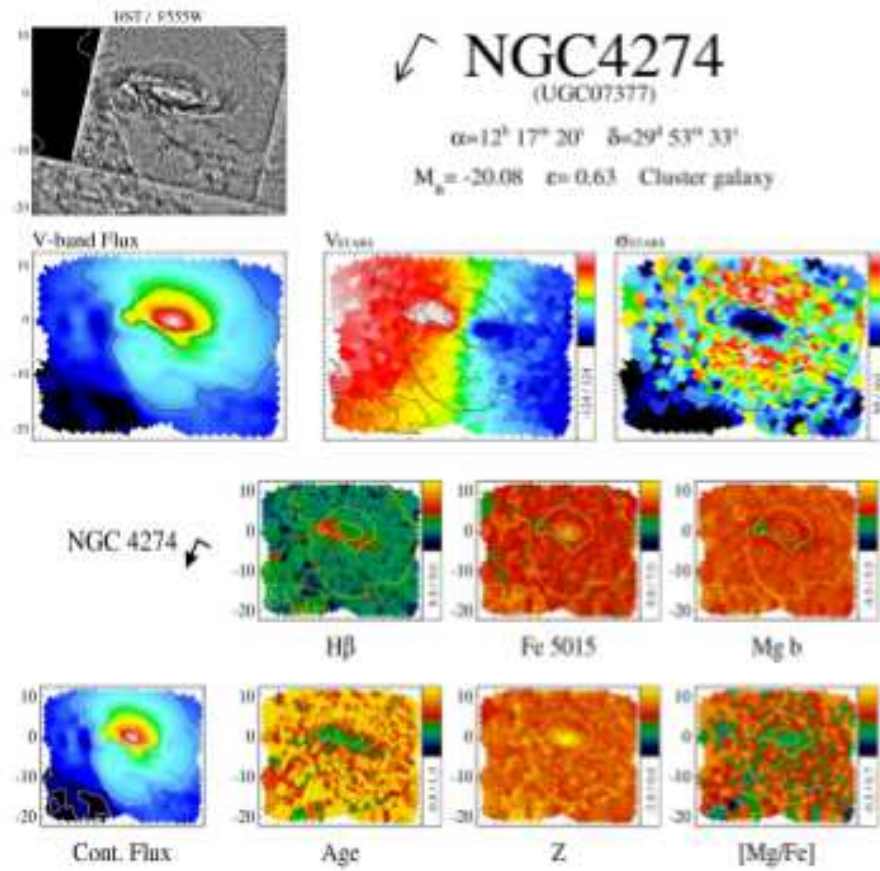


Figure 1.18: Same as Fig.1.17, but now for NGC 4274.

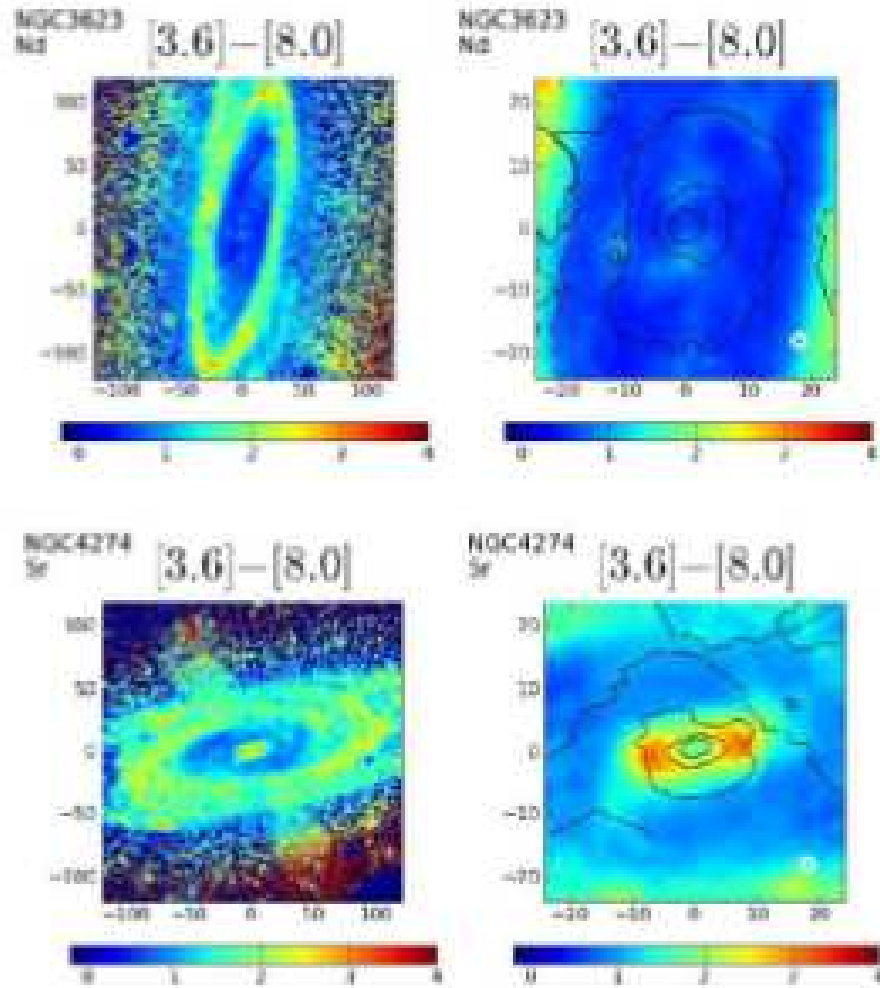


Figure 1.19: Spitzer IRAC [3.6] - [8.0] color maps of the spiral galaxies NGC 3623 and NGC 4273 (from van der Wolk 2011). Shown are color maps of the whole galaxy, and a central zoom. This color, a good indicator of warm dust, shows a considerable amount of dust in the center of NGC 4274, corresponding to the region of the inner spiral in Fig. 1.18 and much less dust in the center of NGC 3623 (Fig.1.17).

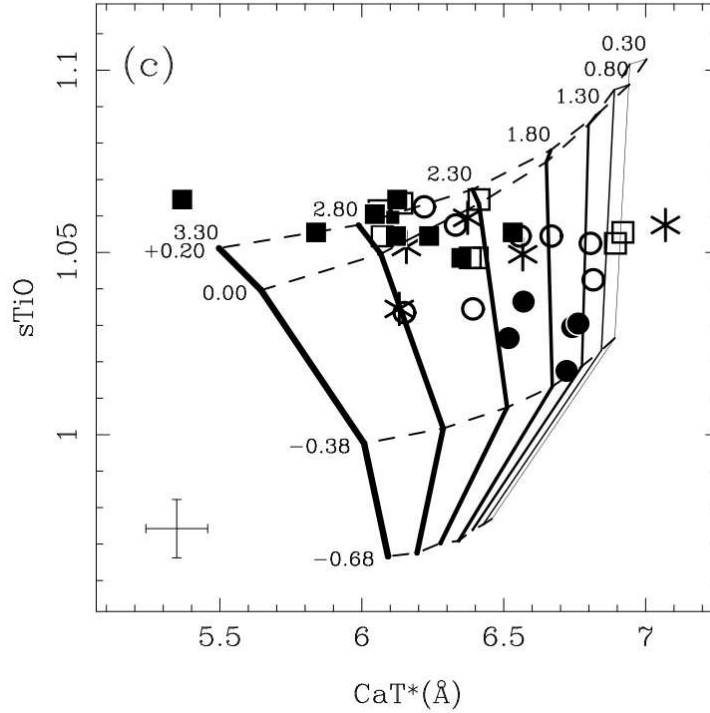


Figure 1.20: SSPs model predictions at fixed old age with varying power-like IMF slopes ($x = 0.3 - 3.3$, see the labels) and metallicity from -0.68 to 0.20 . Different symbols indicate galaxies with different velocity dispersions (see Cenarro et al. 2003).

slope in elliptical galaxies increases for larger galaxies. However, other solutions are possible, e.g., that the $[\text{Ca}/\text{Fe}]$ abundance ratio becomes lower for more massive galaxies. One might also think about systematic errors in the stellar population models that are needed to establish the IMF-slope. For example, in the models that Cenarro et al. use, solar abundance ratios are used in the stellar evolutionary calculations, and the stellar library used mostly consists of stars in the solar neighborhood, which implies that here too the abundance ratios must be close to solar.

Recently, van Dokkum & Conroy (2010, 2011), and Conroy & van Dokkum (2012) have revived this topic. Using new methods to better remove the atmospheric absorption lines and new models in the near-infrared, they present conclusions that the IMF-slope increases with increasing galaxy velocity dispersion (mass). For the largest galaxies the IMFs found are a bit steeper than Salpeter ($x=1.6$). This implies that stellar masses inferred from stellar popula-

tion analysis will have to be increased by a small factor, which will not be larger than 2. Although this is an important result, one should remember the caveat that such a result depends on the stellar population models, which for non-solar abundance ratios are not perfect yet. Similar remarks can be made about the recent paper of Ferreras et al. (2012), who confirm Conroy & van Dokkum's result using the Na doublet at 8200Å with stacked data of a large sample of SDSS galaxies, and of Smith et al. (2012) who use an area near the Wing-Ford band. Recently, Cappellari et al. (2012) claim that independent analysis based on stellar dynamical fits to 2-D kinematic fits to galaxies of the Atlas-3d survey confirms the IMF trends observed in stellar populations.

If, when calculating stellar masses, one still doesn't want to depend on these estimates of the IMF slope, one can also use photometry or indices further to the infrared. For example, it is known that M/L ratios in the K-band vary little with stellar populations, since here the relative contribution to the light of dwarfs vs. giants is much smaller than in the optical. The same holds for the Spitzer [3.6] and [4.5] bands, which are still dominated by light from stars. Meidt et al. (2012) nicely show how stellar masses can be obtained from images in both these bands for spiral galaxies.

1.4.7 Beyond the optical

Stellar population synthesis in the UV is less well developed, because of various reasons. First of all, the amount of data available is limited, since it all has to come from space. Secondly, interpretation is complicated, since a few hot stars can over-shine all other stars, making it very difficult to obtain information on the not so young stellar populations.

Burstein et al. (1988) published a large number of IUE-spectra of early-type galaxies. Their main result was a relation between the 1550 – V color (1550 is here a passband with effective wavelength 1550Å) and the optical Mg₂ index. Massive galaxies with large Mg₂ index have a very blue 1550 – V color. This effect, the so-called UV-upturn, is probably due to extreme horizontal branch stars, but can also have other reasons (see O'Connell 1999 and Yi 2008 for reviews). With new and better quality GALEX-data, Bureau et al. (2011) show that this effect is present only when the optical H β index is low, which implies that from the optical spectrum there is no evidence for any young stellar populations (see Fig. 1.21).

Very little has been done on the analysis of line strength indices. This is surprising, since the UV is particularly important for the analysis of high redshift spectra. Recently, Maraston et al. (2009) published some stellar population models based on the IUE-stellar library of Fanelli et al. (1992). A problem with this empirical library is, that its range in metallicity is small. However, in this region empirical stars are probably more reliable than synthetic spectra, due to difficulties treating the effect of stellar winds that affect the photospheric lines of massive stars. There are still considerable differences between using the Fanelli library and a high-resolution version of the Kurucz library of stellar spectra (Rodríguez-Merino et al. 2005) in the Maraston models.

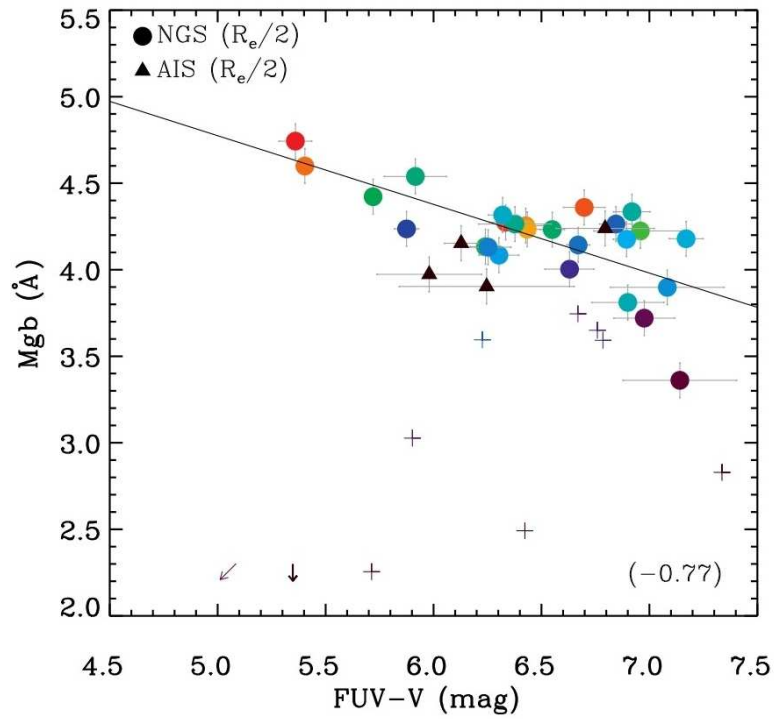


Figure 1.21: Updated FUV - V vs. Mg b diagram (also called Burststein diagram), from Bureau et al. (2011). Galaxies with $H\beta > 1.8 \text{ \AA}$ are indicated with 'plus'-signs.

There are ongoing efforts to develop a stellar library from HST/STIS stars, providing higher S/N and higher resolution spectra than IUE covering a much larger parameter space (the NGSL library - Gregg et al. 2006). This library has not been incorporated into any stellar population models yet, although it has been characterized and stellar parameters have been homogenized in Koleva & Vazdekis (2012).

Just like the UV, the near-IR has also not been studied very much. While broadband colors are predicted by many stellar population models, very few spectrophotometric models are available. The problem has been mentioned before. The NIR is dominated by evolved stellar populations, i.e., RGB and especially AGB, of which the number and lifetimes are not well known, since they are so short-lived that good statistics cannot be obtained from globular and open cluster HR-diagrams. Furthermore, AGB stars lose large amounts of mass, making their lifetimes and also their spectra uncertain. On top of that, they are highly variable. Spectrophotometric models at a resolution of ~ 1100 are available from Mouhcine & Lançon (2002). They are based on about 100 observed stars from Lançon & Wood (2000) for static luminous red stars, stars from Lançon & Mouhcine (2002) for oxygen rich and carbon rich LPVs, and the theoretical library of Lejeune et al. (1997, based on Kurucz models) in all other cases. Conroy & van Dokkum (2012) recently made some models using the IRTF library (Rayner et al. 2009, Cushing et al. 2005). At low resolution ($\sim 50\text{\AA}$), there are models from Maraston (2005) and Charlot & Bruzual (Version of 2007, unpublished), based on theoretical atmospheres, and only tested in the broad bands J, H and K. Maraston also presents some low resolution indices. The problem with the models at present is that only the broad band fluxes have been tested well using clusters and galaxies, but that detailed testing of line indices or narrow band fluxes is still lacking. For example, in a recent paper, Lyubenova et al. (2012) showed that globular clusters cannot be fitted by the models of Maraston (2005) models in the $C_2 - D_{CO}$ diagram. C_2 indicates the line strength of a feature at $1.77\ \mu\text{m}$ (Maraston 2005), while D_{CO} is an index measuring the strength of the CO band head at $2.29\ \mu\text{m}$ (Mármol-Queralto et al. 2008). The problem here is a lack of Carbon stars in the models, stars of ~ 1 Gyr (Lançon et al. 1999). It indicates that making models of the TP-AGB phase is very difficult (see also Marigo 2008). The situation might be improving soon. Better data of nearby galaxies and clusters are becoming available (e.g. Lyubenova et al. 2012, Silva et al. 2008, Mármol-Queralto et al. 2009). And better stellar libraries are expected (e.g., the X-Shooter library (Chen et al. 2011)). By comparing data with models, we will learn where the models should be improved, up to the moment that the NIR will give useful constraints to galaxy evolution theories.

1.4.8 Stellar population analysis from surface brightness fluctuations

In Fig.1.4.8 one sees the nearby dwarf elliptical NGC 205 in 2 bands. In the redder band, F814W, the giants can be distinguished much more easily from

NGC 205 (ACS)

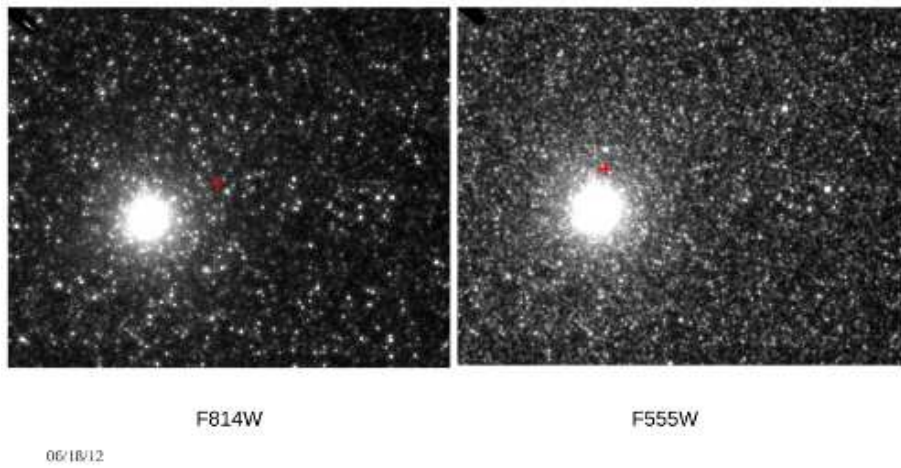


Figure 1.22: The effect of surface brightness fluctuations: ACS images of NGC 205 in F814W (left) and F555W (right).

the underlying mass of fainter stars than in F555W. One can imagine that if this galaxy is placed at larger distances, one can see the individual giants up to larger distances in F814W. One can use the noise map, obtained after removing a smooth model of the galaxy, as a measure of the galaxy distance. Even more, since this noise map strongly depends on the number of bright giants and supergiants, one can use the noise characteristics, or the *surface brightness fluctuations* as a way to characterize the stellar populations in a galaxy.

A review about surface brightness fluctuations as a stellar population indicator is given in Blakeslee (2009). It shows that the method can be used well for determining distances in early-type galaxies (giants or dwarfs), but that the use for stellar population analysis is still limited to the optical. In the near-IR there are considerable discrepancies between surface brightness fluctuations predicted by models and the observations (Lee et al. 2009). With the advent of new, large telescopes, this work will undoubtedly become more important in the future.

1.5 The use of scaling relations

Rather than studying individual galaxies one can also study them by investigating the evolution of so-called scaling relations. Nearby galaxies happen to display clear correlations between well-defined and easily measurable galaxy properties. With high redshift studies now routine, scaling relations are more useful than ever, allowing us to probe the evolution of galaxy populations over a large range of lookback times (e.g. Bell et al. 2004, Saglia et al. 2010). In this review I will discuss the color – (and line strength –) σ relation, a potentially tight relation connecting the galaxy mass to its stellar populations, and the fundamental plane of galaxies, a relation connecting the structure of galaxies to their mass.

1.5.1 The color – σ relation

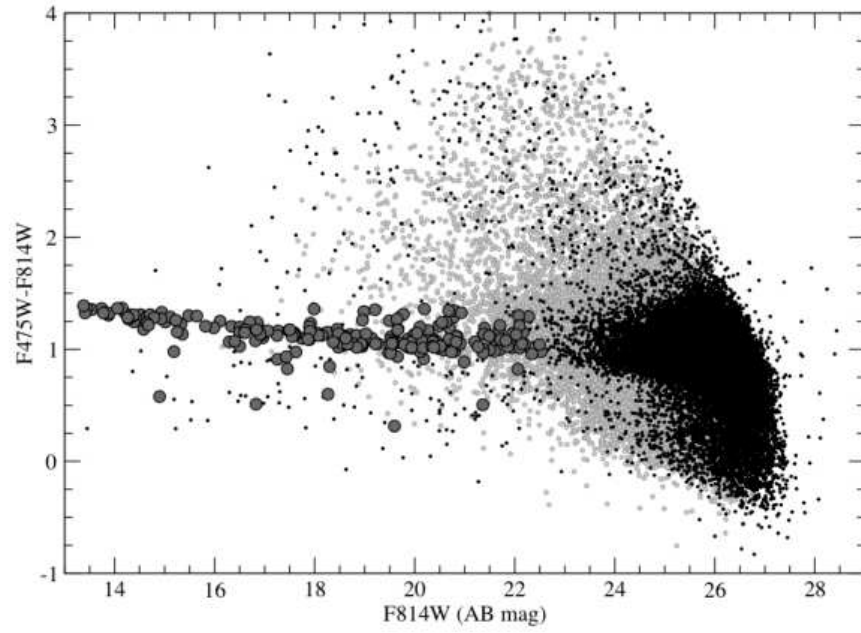
It has been known now for more than 50 years that early-type galaxies show a tight color-magnitude (C-M) relation (Baum 1959, Sandage 1972; Visvanathan & Sandage 1977), in the sense that larger galaxies are redder. Bower et al. (1992) showed that in the Virgo and Coma clusters, when taking small central apertures, the scatter in $U - V$, and $V - K$ is extremely small. Noting that when galaxies age, their color becomes redder, and their velocity dispersion only changes slightly, they could show that cluster ellipticals are made of very old stars, with the bulk of them having formed at $z > 2$. so, by assuming that for a given σ the eldest galaxies are situated at the reddest color, and that along the color – σ relation the metallicity (and possibly also the maximum age for galaxies of a certain σ) changes, one can derive relative ages and metallicities using color – σ relations. It has been used as an important benchmark for theories of galaxy formation and evolution (e.g. Bell et al. 2004; Bernardi et al. 2005) Galaxies devoid of star formation are thought to populate the red sequence, while star-forming galaxies lie in the blue cloud (e.g. Baldry et al.

2004). The dichotomy in the distribution of galaxies in this relation has opened a very productive avenue of research to unravel the epoch of galaxy assembly (e.g. De Lucia et al. 2004; Andreon 2006; Arnouts et al. 2007).

This stellar population – mass relation for galaxies has manifested itself in the literature in many flavors. Various colors have been used, from blue colors that are very age-sensitive to red colors covering a large wavelength baseline (e.g. V-K). To avoid the effects of dust extinction, one often uses line strengths instead of colors. The $\text{Mg}_2 - \sigma$ relation has been used very frequently in the literature (e.g. Terlevich et al. 1981). SDSS related studies have been concentrating on the $\text{H}\delta$ line and the D_{4000} break (Kauffmann et al. 2003), finding that galaxies less massive than $3 \cdot 10^{10} M_{\odot}$ are predominantly younger than more massive galaxies. Cenarro et al. (2003) find an inverse relation of the Ca II IR triplet strength as a function of σ , which up to recently is not well understood, and might have something to do with IMF-changes in galaxies (see Section 1.4.6). The galaxy mass indicator (i.e., here σ) can be replaced by other indicators such as galaxy luminosity, stellar mass, etc. When using stellar mass, the relations are not so tight (e.g. Peletier et al. 2012), since compact ellipticals fall off the relation for the other galaxies. Compact ellipticals have higher σ and also redder colors/line indices than one would expect from their stellar mass. What helps in any case is taking into account both random (σ) and regular motion (rotation) (Zaritsky et al. 2006). This way both ellipticals and spiral galaxies can be compared easily with each other (Falc3n-Barroso et al. 2011). An advantage is that the color – σ relation is independent of galaxy distance. When using mass, or luminosity, the errors involved in measuring these distances will generally dominate the scatter, unless these errors can be avoided, in e.g. a galaxy cluster.

In Fig. 1.23 I show two color – magnitude relations in the Coma cluster. On the right is shown the result of Bower et al. (1999), showing spectroscopically confirmed cluster members. One sees that ellipticals and S0s form a tight color – magnitude relation. Spiral galaxies are bluer for a given magnitude, indicating younger ages. At fainter magnitudes more and more galaxies are falling blueward of the relation, showing that star formation in smaller galaxies is more common. On the left, a diagram is shown from the Coma-ACS survey (Hammer et al. 2010) a survey at a much higher resolution of a small part of the Coma cluster. Many dwarfs are included. At faint magnitudes, many galaxy are shown to be redder or bluer than the linear relation. These are mostly background galaxies, shown by the fact that the larger symbols, the spectroscopically confirmed Coma cluster members, almost all lie on or below the relation. A few compact ellipticals in Coma lie above the relation.

Also for spiral galaxies, the color – σ relation can be used very well to study stellar populations. Falc3n-Barroso et al. (2002) showed that bulges with old stellar populations fall on the tight $\text{Mg b} - \sigma$ relation for elliptical galaxies and S0's. This means that the stellar populations in the bulge of a galaxy is not determined by the mass of the whole galaxy, but by the mass (or σ) of the bulge (similar to the black hole mass - Ferrarese & Merritt 2000). So, by plotting an index, such as Mg b against central σ , one can use the relation in the same way as for ellipticals. In Fig. 1.24 this is done for the spirals of the SAURON survey



The Colour–Magnitude Relation in Coma

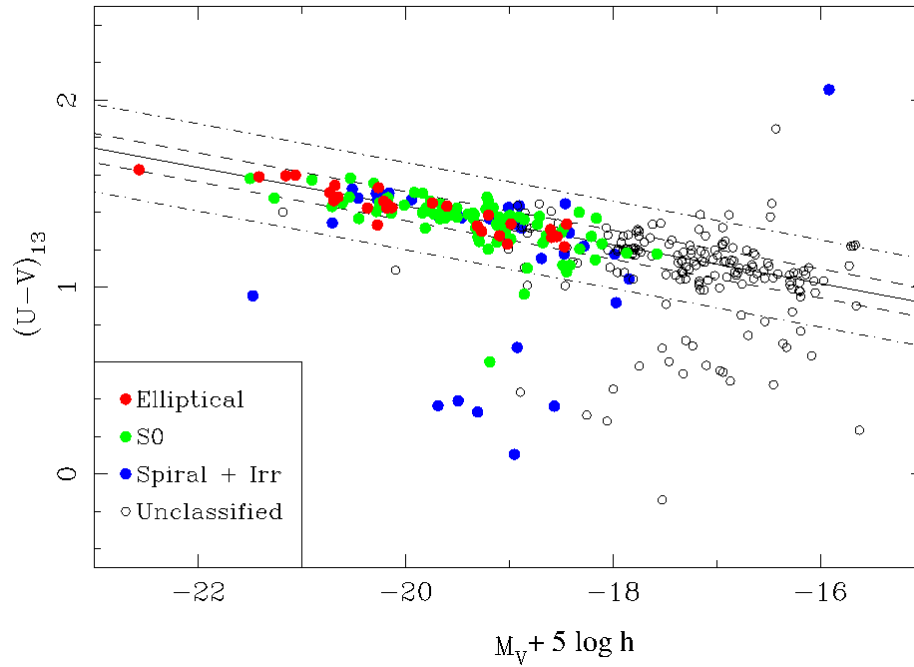


Figure 1.23: The color - magnitude relation in the Coma cluster. Top: $F475W - F814W$ vs. $F814W$ relation from the Coma-ACS survey (Hammer et al. 2010). These apparent magnitudes can be converted to absolute magnitudes using $m - M = 35$. Bottom: $U - V$ vs. M_V relation from Bower et al. (1999).

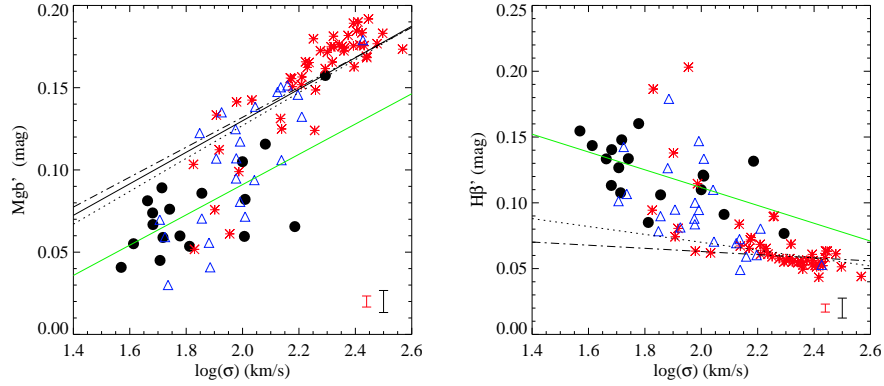


Figure 1.24: $Mg\ b - \sigma$ and $H\beta - \sigma$ relations for 90 ellipticals and bulges from the SAURON sample (from Ganda et al. 2007). Elliptical galaxies are indicated with red asterisks, Sa's with blue open triangles, and later type spirals with filled black circles.

(Peletier et al. 2007, Ganda et al. 2007). Plotted are central line strengths. The figure shows that the central stellar populations in late-type spirals are all younger than the ones in early-type galaxies. Sa's show a large scatter, and have luminosity-weighted stellar populations that range from very young to as old as ellipticals. The diagram on the right, which uses $H\beta$ (in magnitudes) is maybe a better diagram to use, since here the dependence of the index on σ is much lower, which means that one can read off ages much more easily. The $H\beta - \sigma$ diagram has not been used very often in the literature, since only recently one is able to clean the absorption from the $H\beta$ emission. The $H\beta - \sigma$ diagram shows the same results as $Mg\ b - \sigma$: much more scatter in the stellar populations in Sa's (and some small E's and S0's) than in later type galaxies, which, on the other hand, are younger than ellipticals.

1.5.2 Stellar Population Analysis from Spitzer Colors

In recent years the Spitzer Space Telescope has made many observations in 4 bands. The shortest wavelength bands, [3.6] and [4.5], in nearby galaxies are mainly dominated by stellar light, while the [8.0] bands mainly detects warm dust from particles like PAHs (Fazio et al. 2004). Since the light at 3.6 and 4.5 μm is barely affected by extinction, and also not by young, hot stars, the [3.6] - [4.5] color seems to be useful to study the cold stars in early-type galaxies. The color will be affected by AGN and TP-AGB stars, and will also be dependent on metallicity. In Fig.1.25 predictions are shown for the [3.6] - [4.5] color from Marigo et al. (2008) and Charlot & Bruzual (Version of 2007, unpublished) for SSPs of various ages and metallicity. Note that in both sets of models

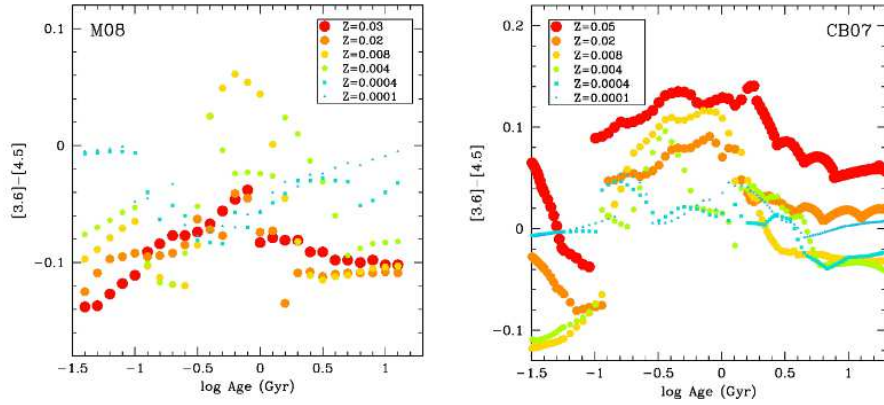


Figure 1.25: SSP Models for $[3.6] - [4.5]$ by Marigo et al. (2008, left) and Charlot & Bruzual (Version of 2007, unpublished) as a function of age and metallicity.

stellar populations of ~ 1 Gyr make this color particularly red ($[3.6] - [4.5]$ goes to larger values). The models do not agree with each other in predicting the dependence of $[3.6] - [4.5]$ as a function of metallicity for old ages: in the Marigo (2008) models $[3.6] - [4.5]$ becomes bluer with increasing metallicity, while in Charlot & Bruzual the colors become redder.

In Peletier et al. (2012) we describe a study of the $[3.6] - [4.5]$ color in the 48 early-type galaxies of the SAURON sample. It is shown that the images in the 2 bands look like smooth, elliptical galaxies in the optical, without dust lanes etc. For every object colors were determined in circular apertures of r_e and $r_e/8$. Also radial color profiles were determined by **1.** Convolution of the $3.6 \mu\text{m}$ image with the $4.5 \mu\text{m}$ PSF and vice-versa, to remove any PSF-effects near the center; **2.** Fitting the same ellipses, with fixed center, ellipticity and position angle in both bands; **3.** Performing accurate sky subtraction; and **4.** Making the ratio of both profiles. One color profile is shown in Fig.1.26, where we show the (optical) SAURON continuum image, the $H\beta$ absorption map, and the $[3.6] - [4.5]$ color profile. The high values in the $H\beta$ map show the stellar populations in the dust lane, which are younger than in the main galaxy. The $[3.6] - [4.5]$ profile shows that these young stellar populations make the color redder. On top of that, the general gradient is making the galaxy slowly redder when going outwards. Given the fact that most galaxies become less metal rich going outward, this might mean that $[3.6] - [4.5]$ becomes redder for decreasing metallicity, or bluer for increasing metallicity. We can understand this when we know that the $4.5 \mu\text{m}$ band contains a large CO absorption band. When the metallicity increases, this band gets stronger, making $[3.6] - [4.5]$ bluer (see Peletier et al. 2012).

Most galaxies have colors everywhere between -0.15 and 0. An exception is M 87, the central Virgo galaxy, which has a very red center, due to the synchrotron emission in center and jet. No other galaxies contain such prominent

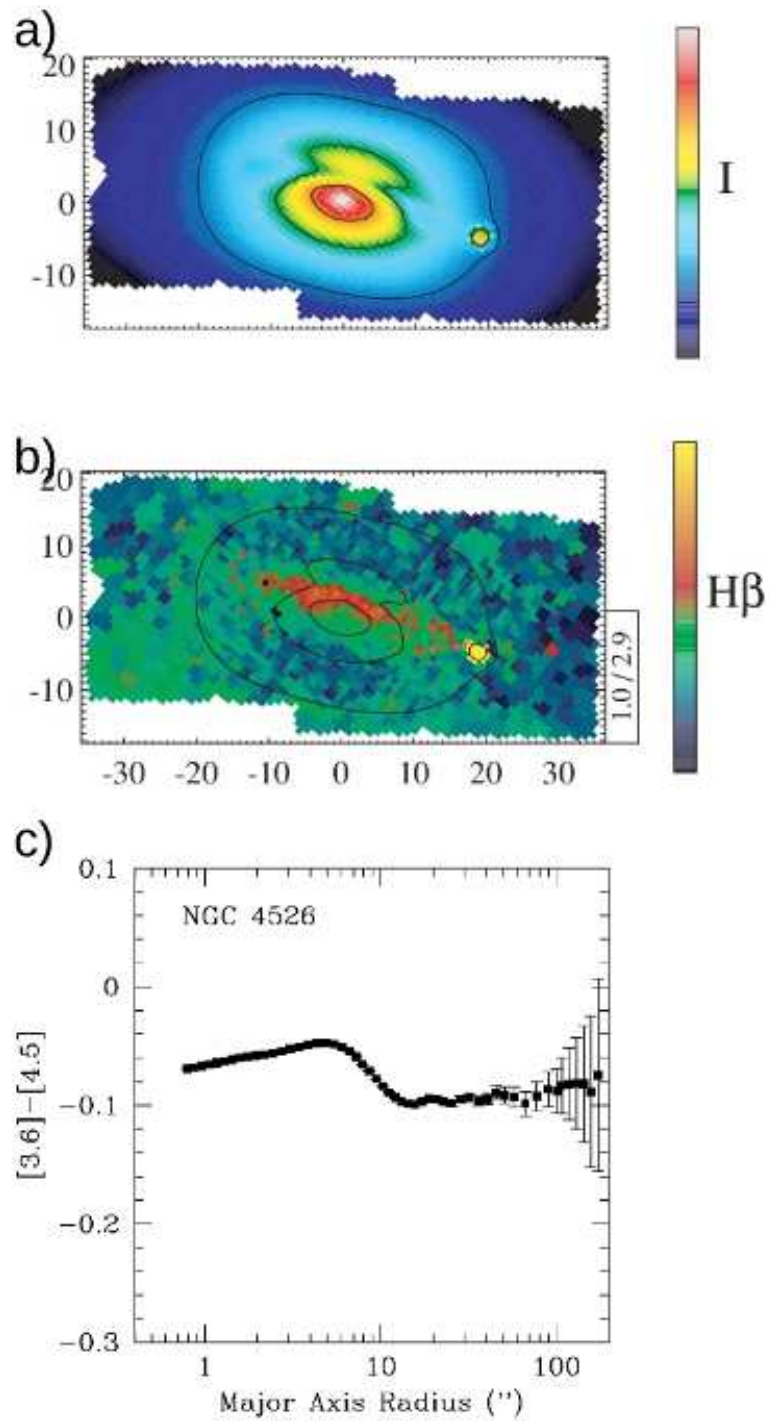


Figure 1.26: SAURON images in V-band continuum (a)) and H β absorption for NGC 4526. The yellow spot is a foreground star. In the bottom panel is shown the [3.6] - [4.5] profile. The central redder part of the profile corresponds exactly to the inner disk seen in the upper 2 panels (from Peletier et al. 2012).

central point sources. When plotting the relation of $[3.6] - [4.5]$ and σ (Fig.1.27) we see that both quantities are strongly related. In this diagram we have colored the galaxies with their age inside $r_e/8$, as obtained by Kuntschner et al. (2010) from the SAURON line indices. Had we used ages within r_e , the figure would have been similar, but with a smaller range in colors. This is because in these early-type galaxies many more young features are seen in the inner parts than further out. The color – σ relation shows that more massive galaxies are bluer. The color coding of the figure shows that these galaxies are at the same time older, if one considers the luminosity-weighted SSP-ages. The main difference with other colors is that the $[3.6] - [4.5]$ color becomes *bluer* for increasing galaxy mass/luminosity.

So, what is the origin of this color – σ relation? Here one has to use mainly empirical arguments, since the models still are rather uncertain. One could think that metallicity is the main driver, with galaxies becoming less metal rich for decreasing σ , and as a result redder. On the other hand, one does not know what the metallicity dependence of $[3.6] - [4.5]$ is. One could also think that age is the dominant driver. In this case the fraction of AGB stars has to increase with decreasing σ . Since these stars are red, the galaxy colors then become redder. If this proves to be true, this would be a promising way to determine the contribution from AGB stars in galaxies. If the scatter in the color – σ relation can be explained by young stellar populations on top of a much older underlying stellar population, one would expect the outliers of the optical line strength – σ relations of Kuntschner et al. (2006) to be the same as the outliers of the color – σ relation here. A close look teaches us that this is to first order the case. Also, there is a strong correlation between Mg b and $[3.6] - [4.5]$. If the color – σ relation is driven by age, it would mean that the young populations that are responsible for the bluing of $[3.6] - [4.5]$ are also responsible both for the decreasing Mg b and increasing $H\beta$ index. Although it is hard to quantify what kind of SSP would be needed, the strong correlation between Mg b, which is sensitive for stellar populations from 10^{6-7} y, and $[3.6] - [4.5]$, which is mostly sensitive to stars above $3 \cdot 10^8$ y, would indicate that stellar populations in these galaxies would have ages older than $3 \cdot 10^8$ y. This is not very realistic, since the galaxies that are blue in the $[3.6] - [4.5] - \sigma$ relation always show $H\beta$ *emission* lines in the region of the young stars, indicating recent star formation. The alternative would be that AGB-populations are much less important than people think. That would agree with recent results from Zibetti et al. (2012), who, from near-infrared spectroscopy of post-starburst galaxies, find a much lower contribution from AGB stars than is expected from the *TP-AGB heavy* models of Maraston (2005). More research clearly is needed to understand the contribution of this evolved stellar population in galaxies.

1.5.3 The fundamental plane of galaxies

Since its discovery (Djorgovski & Davis 1987; Dressler et al. 1987), the Fundamental Plane (FP) has been one of the most studied relations in the literature. Given its tightness, like many other scaling relations the FP was quickly envis-

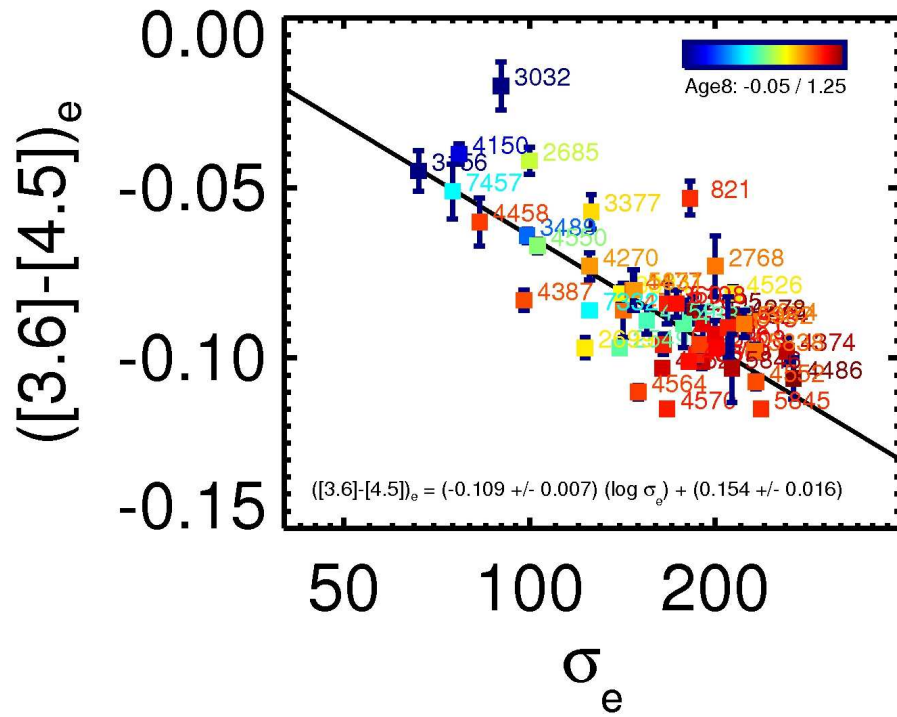


Figure 1.27: $[3.6] - [4.5]$ color as a function of velocity dispersion in km/s. The velocity dispersion has been measured within r_e . Here the color, determined within 1 effective radius, is shown.

aged as a distance estimator as well as a correlation to understand how galaxies form and evolve (e.g. Bender, Burstein & Faber 1992 (BBF), Jørgensen et al. 1996; Pahre et al. 1998; Bernardi et al. 2003). It is widely recognized that the FP is a manifestation of the virial theorem for self-gravitating systems averaged over space and time with physical quantities total mass, velocity dispersion, and gravitational radius replaced by the observables mean effective surface brightness μ_e , effective (half-light) radius (r_e), and stellar velocity dispersion σ . Since velocity dispersion and surface brightness are distance-independent quantities, contrary to effective radius, it is common to express the FP as $\log(r_e) = \alpha \log(\sigma) + \beta \mu_e + \gamma$, to separate distance-errors from others. If galaxies were homologous with constant total mass-to-light ratios, the FP would be equivalent to the virial plane and be infinitely thin, with slopes $\alpha = 2$ and $\beta = 0.4$. By studying the intrinsic scatter around the FP, one can study how galaxy properties differ within the observed sample.

Just like the color – σ relation, the FP is a very useful tool to study the evolution of stellar populations. To first order approximation, radius and σ are independent of stellar populations, while μ_e is. If a stellar population ages, its luminosity decreases, and therefore also its surface brightness. However, if one studies the evolution with redshift, one also has to take into account the fact that galaxies become more compact with redshift (radius evolution), and consequently their velocity dispersion increases as well.

An important study to mention here is the EDisCS study of the FP of galaxies in clusters up to $z=0.9$ (Saglia et al. 2010). Combining structural parameters from HST and VLT images and velocity dispersions from VLT spectra, they have been able to determine Fundamental Plane fits for clusters with a range in redshift, as well as for galaxies in the field. At face-value, on average, the evolution of the surface brightness follows the predictions of simple stellar population models with high formation redshift ($\sim z = 2$) for all clusters, independent of their total mass (see Fig. 1.28). However, it looks as if both the evolution of early-type galaxies with redshift and the dependence of this evolution on environment differ for galaxies of different mass. These differences manifest themselves as an evolution in the FP coefficient α as a function of redshift. They also find size and velocity dispersion evolution of the sample. However, after taking into account the progenitor bias affecting the sample (large galaxies that joined the local early-type class only recently will progressively disappear in higher redshift samples), the effective size and velocity dispersion evolution reduce substantially. So after making corrections for radius and velocity dispersion evolution, they found, using SSP models, that massive ($M > 10^{11} M_\odot$) cluster galaxies are old, with formation redshifts $z > 1.5$. In contrast, lower mass galaxies are just 2 to 3 Gyr old. This agrees with the EDisCS results from colors and line strength (e.g. Poggianti et al. 2006) who argue that the lower luminosity, lower mass population of early-type galaxies comes in place only at later stages in clusters. Field galaxies follow the same trend, but are ~ 1 Gyr younger at a given redshift and mass. This picture in principle is in agreement with the picture one gets from stellar population analysis of nearby galaxies (Thomas et al. 2005).

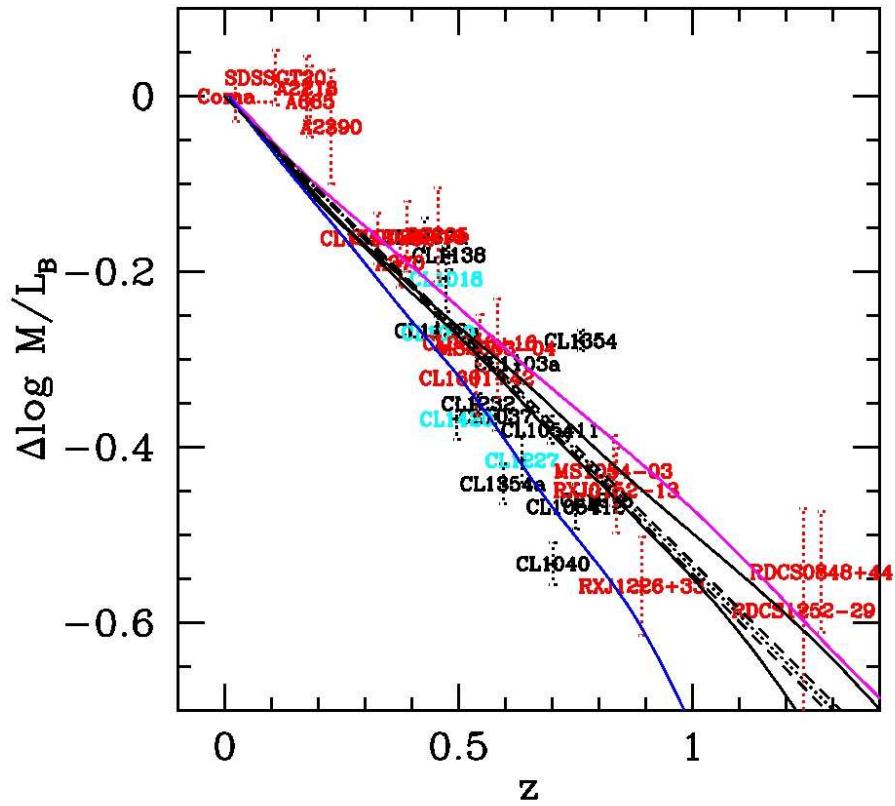


Figure 1.28: Redshift evolution of the B band mass-to-light ratio (from Saglia et al. 2010). The full black lines show the simple stellar population (SSP) predictions for a Salpeter IMF and formation redshift of either $z_f = 2$ (lower) or 2.5 (upper curve) and solar metallicity from Maraston (2005). The blue line shows the SSP for $z_f = 1.5$ and twice-solar metallicity, the magenta line the SSP for $z_f = 2.5$ and half-solar metallicity. The dotted line shows the best-fit linear relation and the σ errors dashed.

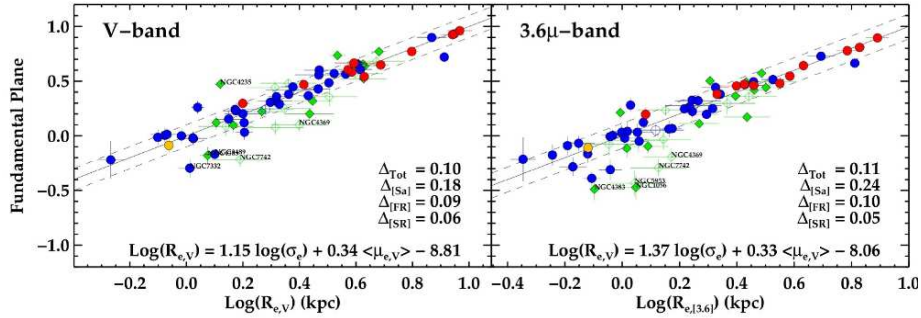


Figure 1.29: Edge-on views of the Fundamental Plane relation for the galaxies in the SAURON sample of galaxies in V - and $3.6\mu\text{m}$ -bands. Circles denote E/S0 galaxies, diamonds Sa galaxies. Filled symbols indicate galaxies with good distance estimates, open symbols those with only recession velocity determinations. In blue we highlight Fast Rotators, in red Slow Rotators and in green the Sa galaxies. The special case of NGC4550, with two similarly-massive counter-rotating disc-like components, is marked in yellow. The solid line is the best fit relation (as indicated in the equation in each panel) (from Falc3n-Barroso et al. 2011).

In the local Universe, the high S/N of the observations make it possible to look at the FP in more detail. Here we can study the position of bulges on the FP (e.g. Bender et al. 1992, Falc3n-Barroso et al. 2002), the scatter in the stellar population ages of galaxies, the amount of dark matter in various types of galaxies along the FP, etc. Falc3n-Barroso et al. (2011) (Fig. 1.29) studied the FP for the SAURON sample of 48 E/S0 galaxies and 24 Sa's. To avoid the effects of internal extinction in galaxies, they use the Spitzer $3.6\mu\text{m}$ band. The velocity dispersion they use is the dispersion calculated using the integrated spectrum inside 1 effective radius. If measured in this way, it includes both rotation and random motions (Zaritsky et al. 2006), and both ellipticals and spirals can be put on the same diagram. Falc3n-Barroso et al. find that the SAURON slow rotators (SR, Emsellem et al. 2007) define a very tight FP, tighter than the fast rotators. This confirms the study from colors and line indices that SR are uniformly old systems, although it also shows that slow rotators have the same homology (radius - surface brightness - mass relations). In the V-band the spiral galaxies deviate because of younger stellar populations, but also because of extinction, two effects which work in opposite directions.

If one goes down in mass towards dwarf galaxies, one traditionally finds that dwarf ellipticals lie above the fundamental plane (BBF, de Rijcke et al. 2005). Converting the FP-parameters into new parameters κ_1 , κ_2 and κ_3 using a coordinate transformation (from BBF), one can directly see how the mass ($\propto \kappa_1$) and M/L ($\propto \kappa_3$) evolve. If one does this, one finds that dwarf ellipticals have higher M/L ratios than ellipticals and S0's on the fundamental plane. This result has

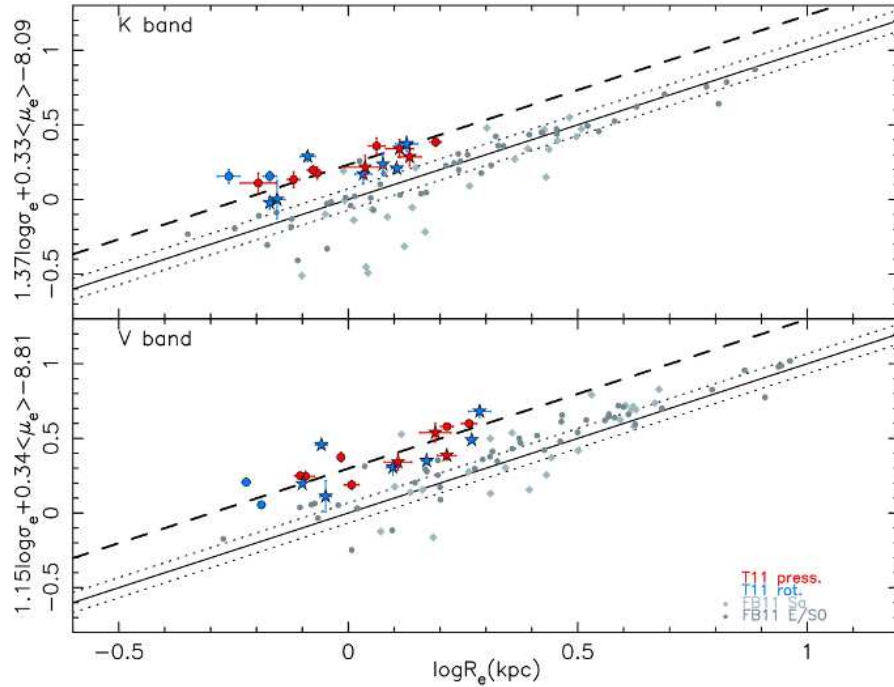


Figure 1.30: The position of dwarf ellipticals on FP (from Toloba et al. 2012). The early-type galaxies and Sa's are from Falcón-Barroso et al. 2011. Shown in red are rotationally supported dwarfs, and in blue pressure supported ones. Note that the dwarfs lie predominantly above the large galaxies, showing intrinsically higher dark matter fractions.

been revised recently using Toloba et al. (2012), who obtained high quality data for a larger sample of dwarfs (some supported by rotation and some by random motions). From their long-slit data they simulated the integrated spectrum inside an effective radius, to determine the generalized dispersion (Zaritsky et al. 2006) also for the dwarfs. They show that also the new data for dwarf galaxies fall above the fundamental plane. Correcting for the effects of stellar populations using line indices from Michielsen et al. (2008) in the way described by Graves & Faber (2010) they find that the objects remain above the FP, and have dynamical to stellar mass ratios around 1.5 (see Fig.1.30). If one, however, goes down to even lower mass dwarfs, these ratios rise to much higher values (Wolf et al. 2010).

1.6 Stellar Population gradients in early-type galaxies

Metallicity gradients provide a means of studying galaxy formation. Classical monolithic collapse scenarios (Larson 1974; Carlberg 1984) predict strong metallicity gradients. In this scenario primordial clouds of gas sink to the center of an over density where a rapid burst of star formation occurs. In-falling gas mixes with enriched material freed from stars by stellar evolutionary processes and forms a more metal rich population. Because the gas clearing time (and hence the number of generations which enrich the interstellar medium) is dependent on the depth of the potential well, the metallicity gradient is dependent on the mass of the galaxy. Mergers, dominant in hierarchical galaxy formation scenarios, will dilute existing population gradients (e.g. White 1980; di Matteo et al. 2009), although residual central star formation can steepen gradients again (e.g. Hopkins et al. 2009, among others). Therefore, the study of metallicity gradients can be used to distinguish between competing scenarios of galaxy formation and can eventually lead to a more detailed understanding of those scenarios. Many attempts have been made to model metallicity gradients in more detail (e.g., Kawata & Gibson 2003, Kobayashi 2004; Pipino et al. 2010). They are generally able to reproduce the gradients, but the predictive power of the models at present is low.

Here I would like to discuss some new work on the gradient vs. mass relation, which might lead to a better understanding of this relation, and therefore galaxy formation. Using the 3 (sometimes 4) SAURON line strength indices Kuntschner et al. (2010) have derived metallicity- and age gradients in their 48 early-type galaxies. Note that they did this assuming that at every position the stellar populations were represented by an SSP. The resulting profiles are shown in Fig.1.31. The color of the galaxies corresponds to the central age. One sees that galaxies become more metal poor going outward slowly, with little difference between the gradients of the individual galaxies. This picture is consistent with the literature (e.g. Davies et al. 1993, Carollo & Danziger 1993). At the same time $[\alpha/\text{Fe}]$ does not change very much as a function of radius in the galaxy. The most striking of this figure are the age profiles. There are many galaxies which are old everywhere. These generally are the Slow Rotators (see Section 1.5.3), which is probably the reason their scatter in the FP is so small. Many other galaxies are younger in the central regions. These regions correspond to central disks, which are very common not only in early-type galaxies, but also in spirals. Note that although many central disks are younger, there are also central disks which are just as old as the rest of the galaxy. This figure is very instructive. It tells us that if we want to investigate the metallicity gradient in galaxies, there is no point in considering these inner regions, since here almost certainly the SSP-approximation is unjustified, so that the luminosity-weighted metallicity is probably very uncertain. To verify this, in Fig.1.32 we plot the metallicity gradients of Kuntschner et al. (2010) against the Spitzer [3.6] – [4.5] color gradients (see Section 1.5.2). We see a good correlation for the old

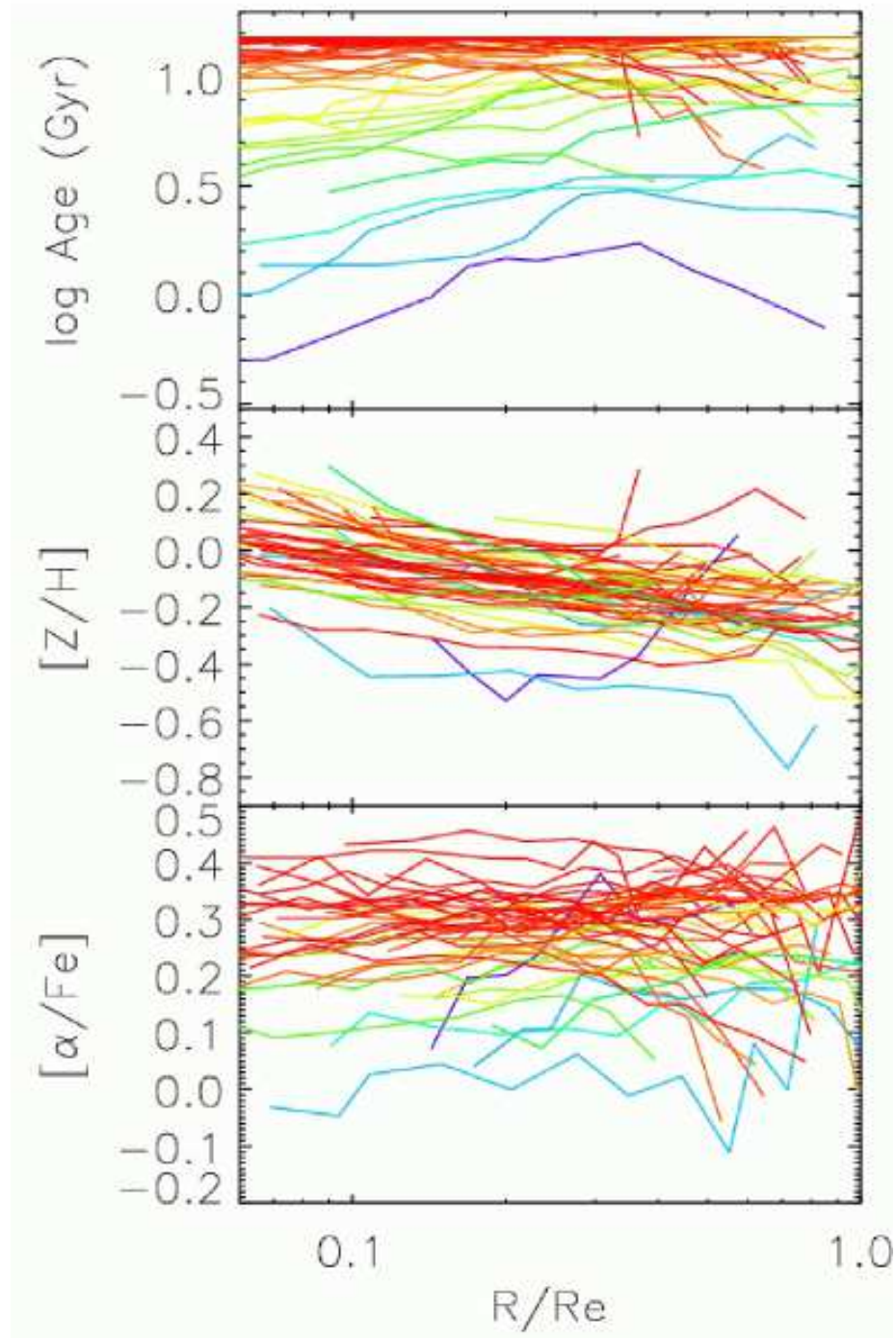


Figure 1.31: Overview of radial profiles, averaged along isophotes, of luminosity weighted age, metallicity and $[\alpha/Fe]$ for the 48 early-type galaxies in the SAURON sample. The color coding reflects central $r_e/8$ SSP-equivalent age with red referring to old stellar populations and blue to young ones (see top plot) (from Kuntschner et al. 2010).

galaxies, but for galaxies with young central ages, the correlation breaks down. Although we have tried in Peletier et al. (2012) not to use the inner, younger, region to fit the gradients, this approach is difficult, and tricky (see Fig. 1.31). On the other hand, the good correlation in Fig. 1.32 shows that the $[3.6] - [4.5]$ color probably has a strong metallicity dependence.

Plotting now these gradients against mass in Fig. 1.32 (right) we see no relation between the two quantities, except that the gradients for the old galaxies are mostly between 0.05 and 0.10.

Realizing this problem with the SSP-based interpretation, we now turn to dwarf ellipticals. Spolaor et al. (2009) showed a very strong correlation between gradient and mass in the mass range between $3 \cdot 10^9$ and $3 \cdot 10^{10} M_{\odot}$, albeit with very few galaxies. Gradients become weaker when going to smaller galaxies, even becoming positive, indicating positive metallicity gradients. This would have strong implications on e.g. the effects of galactic SN-driven winds. In den Brok et al. (2011) we have investigated this effect in detail. We have determined color gradients for a sample of dwarf galaxies in the Coma cluster using the Coma-ACS survey. In this rich cluster environment the number of young stars in galaxies is minimized, which means that it is easier to study metallicity gradients. It turns out that the central regions here are strongly influenced by small central, younger regions, so-called nuclear clusters. Since many dwarf ellipticals have nuclear clusters, this effect is very important. In Fig. 1.6 I show that the gradient – mass relation before and after removing the nuclear clusters. In the second case, we indeed find a relation of gradients with mass. Going to smaller galaxies, the gradients (per dex in radius) become smaller, but remain negative, in agreement with galaxy formation models. For large galaxies one sees a large scatter in the gradients. Only compact ellipticals do not obey the gradient - mass relation. They behave in many ways as the central regions of much larger galaxies.

Given the poor reproduction of gradients by simulations, we can only speculate what these results mean in terms of galaxy formation models. The observed trends with galaxy mass imply that somehow the mass of the galaxy, or the potential well are important in shaping the gradient (see also the $Mg\ b - v_{esc}$ relation (Scott et al. 2009). However, given the scatter in gradients at a given magnitude, this cannot be the only important process. Another clue comes from the Sérsic index – gradient relation. Galaxies with nearly exponential profiles have flatter gradients than galaxies with higher Sérsic indices (den Brok et al. 2011). Higher Sérsic indices are thought to be the results of processes involving violent relaxation. Since this is a non-dissipational process by itself, the strong gradients may point at a history of moist or wet mergers.

1.7 Future prospects

The field of stellar populations is very much alive, and will stay alive for a long time to go, since it is by far the most accessible way to study galaxies in the very distant Universe. Led by the Hubble Space Telescope, we know much more

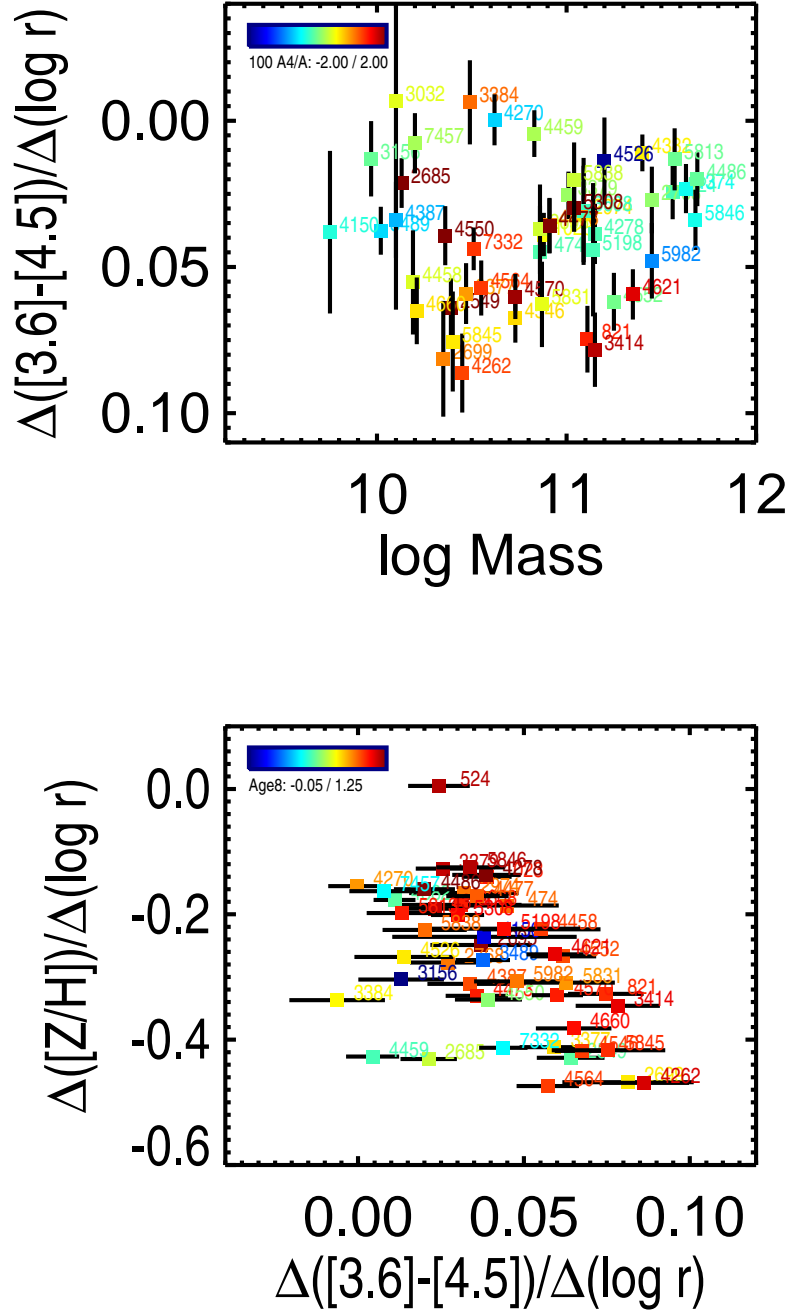


Figure 1.32: Top: SAURON metallicity gradients (from Kuntschner et al. 2010) as a function of the [3.6] – [4.5] gradient (from Peletier et al. 2012). The coloring of the points is done according to the central age. Bottom: [3.6] – [4.5] gradient as a function of mass.

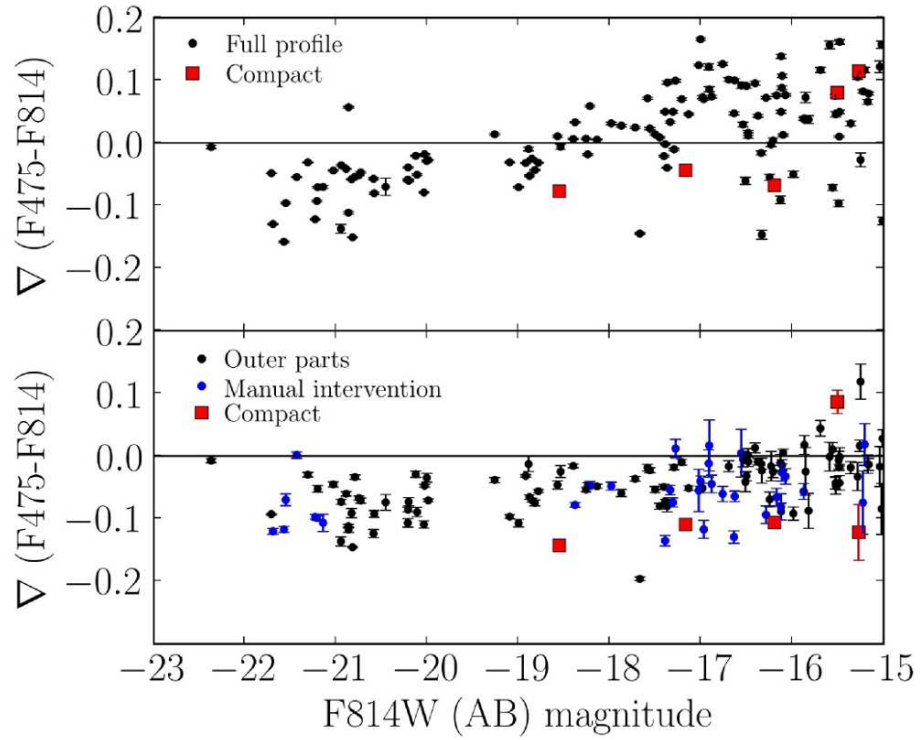


Figure 1.33: Top: Color gradients of likely Coma members as a function of absolute magnitude. Bottom: Color gradients of the same galaxies, now excluding the central parts from the fit. Red squares are compact galaxies from Price et al. (2009). The blue points required manual intervention. (From den Brok et al. 2011).

about the Star Formation History of the Universe than 10 years ago. However, as far as the interpretation of observations of galaxies at very high redshifts is concerned, stellar population modelling lies far behind observations, and it is very important that we make a huge effort together to catch up. This mainly involves the modelling in the NUV and FUV, where just a few stars dominate the integrated stellar populations. Also other areas need work: a lot of effort is needed in the near-IR, to understand better how stars evolve, so that we can use near-IR features to study the evolution of galaxies. For a few other challenges, I refer to the excellent list by Brinchmann (2010). To these I add the understanding of abundance ratios in galaxies. We are slowly getting ready to apply the techniques that have been so powerful for resolved galaxies to integrated spectra. Interpreting abundance ratios will give us another dimension that will help us to solve the puzzle of galaxy evolution. Abundance ratios affect everything. The fact that they also affect broadband colors (Ricciardelli & Vazdekis 2012) shows that also photometric redshifts will suffer from systematic errors. Another issue is the IMF, which at the moment is popular again. Understanding the dark matter in galaxies, and therefore also the stellar mass, is fundamental. It is still very difficult to derive accurate stellar masses of galaxies, but we are making progress. The main difference with the past is we now have new observations from gravitational lensing which independently can constrain the IMF slope.

In the future there will be many new facilities useful for stellar population studies. A few examples, ranked by increasing telescope size, are X-shooter on the VLT, the JWST and the E-ELT. They will give the high spectral resolution and the high signal-to-noise needed to derive accurate star formation histories which can be combined with high resolution LOSVDs. They will open new fields, such as the redshifted optical and near-IR. At the same time GAIA will determine the stellar populations in our Galaxy in much more detail as before, so that we can use the Milky Way as template for studies of other galaxies.

The fact that more and more data is available of always higher quality is also reflected in an increasing popularity of the field of stellar populations within the astronomical community (see Fig. 1.34). Brinchmann (2010) shows that many astronomers feel interested in helping to solve the problems in the field of stellar populations. I am sure that a lot of progress will come from you, the attendants of the Winter School.

I would like to finish this review with a quote of Renzini (2006): *Baryon physics, including star formation, black hole formation and their feedbacks, is highly nonlinear, and it is no surprise if modeling of galaxy evolution relies heavily on many heuristic algorithms, their parameterization, and trials and errors. Dark matter physics, on the contrary, is extremely simple by comparison. Thus, the vindication of the CDM paradigm should be found in observations demonstrating that the biggest, most massive galaxies are the first to disappear when going to higher and higher redshifts. This is indeed what has not been seen yet, and actually there may be hints for the contrary.* This statement is probably supported by Tolstoy et al. (2009): *The hierarchical theory of galaxy formation contains at its heart the concept of smaller systems continuously merging*

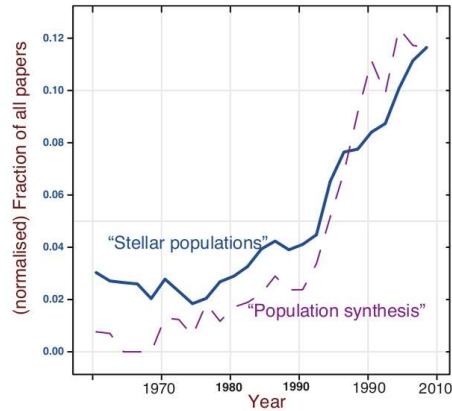


Figure 1.34: The fraction of papers in A&A, AJ, ApJ and MNRAS each year that mention *Stellar populations* (solid line) or *Population synthesis* (dashed line, scaled up by a factor of 8) in their abstracts. Currently about 12% of all papers mention *Stellar populations*. (from Brinchmann 2010).

to form larger ones. This leads to the general expectation that the properties of the smaller systems will be reflected in the larger. (...) From recent abundance studies of low-metallicity stars in dSphs, it seems likely that there exist only narrow windows of opportunity when the merging of dwarf galaxies to form larger systems would not lead to inconsistencies. The biggest challenge for the future is to connect baryon and dark matter physics. But finding the solution here obviously is not so easy.

Acknowledgments

I thank Johan Knapen and Jesús Falcón-Barroso for having organized a very interesting and pleasant meeting, and the IAC secretaries for making sure that everything ran smoothly.

Bibliography

- Andreon, S. 2006, MNRAS, 369, 969
- Arimoto N., Yoshii Y., 1987, AAP, 173, 23
- Arnouts, S., Walcher, C. J., Le Fèvre, O., et al. 2007, A&A, 476, 137
- Ashman, K. M., & Zepf, S. E. 1992, ApJ, 384, 50
- Baade, W. 1944, ApJ, 100, 137
- Bacon, R., Copin, Y., Monnet, G., et al. 2001, MNRAS, 326, 23
- Bagnulo, S., Jehin, E., Ledoux, C., et al. 2003, The Messenger, 114, 10
- Balcells, M., & Peletier, R. F. 1994, AJ, 107, 135
- Baldry I. K., Glazebrook K., Brinkmann J., Ivezić Ž., Lupton R. H., Nichol R. C., Szalay A. S., 2004, ApJ, 600, 681
- Bastian, N., Covey, K. R., & Meyer, M. R. 2010, ARAA, 48, 339
- Baum W. A., 1959, PASP, 71, 106
- Bell, E. F., & de Jong, R. S. 2001, ApJ, 550, 212
- Bell, E. F., Wolf, C., Meisenheimer, K., et al. 2004, ApJ, 608, 752
- Bender R., Burstein D., Faber S. M., 1992, ApJ, 399, 462
- Bernardi M., et al., 2003, AJ, 125, 1882
- Bernardi, M., Sheth, R. K., Nichol, R. C., Schneider, D. P., & Brinkmann, J. 2005, AJ, 129, 61
- Bica, E. 1988, A&A, 195, 76
- Blakeslee, J. P. 2009, American Institute of Physics Conference Series, 1111, 27
- Bland-Hawthorn, J., Vlajić, M., Freeman, K. C., & Draine, B. T. 2005, ApJ, 629, 239

- Bond, H. E., & MacConnell, D. J. 1971, *ApJ*, 165, 51
- Bower R. G., Lucey J. R., Ellis R. S., 1992, *MNRAS*, 254, 601
- Bower, R. G., Terlevich, A., Kodama, T., & Caldwell, N. 1999, *Star Formation in Early Type Galaxies*, 163, 211
- Brinchmann, J. 2010, *IAU Symposium*, 262, 3
- Bruzual G., Charlot S., 2003, *MNRAS*, 344, 1000
- Bureau, M., Jeong, H., Yi, S. K., et al. 2011, *MNRAS*, 414, 1887
- Burstein, D., Faber, S. M., Gaskell, C. M., & Krumm, N. 1984, *ApJ*, 287, 586
- Burstein, D., Bertola, F., Buson, L. M., Faber, S. M., & Lauer, T. R. 1988, *ApJ*, 328, 440
- Cappellari, M., McDermid, R. M., Alatalo, K., et al. 2012, *Nature*, 484, 485
- Cardelli, J. A., Clayton, G. C., & Mathis, J. S. 1989, *ApJ*, 345, 245
- Carlberg R. G., 1984, *ApJ*, 286, 403
- Carollo, C. M., Danziger, I. J., & Buson, L. 1993, *MNRAS*, 265, 553
- Carter, D., Visvanathan, N., & Pickles, A. J. 1986, *ApJ*, 311, 637
- Cenarro A. J., Gorgas J., Vazdekis A., Cardiel N., Peletier R. F., 2003, *MNRAS*, 339, L12
- Cenarro, A. J., Cardiel, N., Gorgas, J., et al. 2001, *MNRAS*, 326, 959
- Chabrier, G. 2003, *PASP*, 115, 763
- Charlot, S., Worthey, G., & Bressan, A. 1996, *ApJ*, 457, 625
- Chen, Y., Trager, S., Peletier, R., & Lançon, A. 2011, *Journal of Physics Conference Series*, 328, 012023
- Chies-Santos, A. L., Larsen, S. S., Cantiello, M., et al. 2012, *A&A*, 539, A54
- Cid Fernandes, R., Mateus, A., Sodré, L., Stasińska, G., & Gomes, J. M. 2005, *MNRAS*, 358, 363
- Clarkson, W. I., Sahu, K. C., Anderson, J., et al. 2011, *ApJ*, 735, 37
- Coelho, P. 2009, *American Institute of Physics Conference Series*, 1111, 67
- Coelho, P., Bruzual, G., Charlot, S., et al. 2007, *MNRAS*, 382, 498
- Cole, A. A., Skillman, E. D., Tolstoy, E., et al. 2007, *ApJ*, 659, L17
- Conroy, C., & van Dokkum, P. 2012, *ApJ*, 749, 95

- Cushing, M. C., Rayner, J. T., & Vacca, W. D. 2005, *ApJ*, 623, 1115
- Dalcanton, J. J., Williams, B. F., Seth, A. C., et al. 2009, *ApJs*, 183, 67
- Davies, R. L., Sadler, E. M., & Peletier, R. F. 1993, *MNRAS*, 262, 650
- de Zeeuw P. T., et al., 2002, *MNRAS*, 329, 513
- De Lucia, G., Kauffmann, G., Springel, V., et al. 2004, *MNRAS*, 348, 333
- den Brok, M., et al. 2011, *MNRAS*, 653
- de Rijcke, S., Michielsen, D., Dejonghe, H., Zeilinger, W. W., & Hau, G. K. T. 2005, *A&A*, 438, 491
- di Matteo P., Pipino A., Lehnert M. D., Combes F., Semelin B., 2009, *AAP*, 499, 427
- Djorgovski, S., & Davis, M. 1987, *ApJ*, 313, 59
- Dotter, A., Chaboyer, B., Ferguson, J. W., et al. 2007, *ApJ*, 666, 403
- Dressler, A. 1980, *ApJ*, 236, 351
- Dressler, A., Faber, S. M., Burstein, D., et al. 1987, *ApJl*, 313, L37
- Eddington, A. S. 1926, *The Internal Constitution of the Stars*, Cambridge: Cambridge University Press, 1926. ISBN 9780521337083.,
- Edvardsson, B., Andersen, J., Gustafsson, B., et al. 1993, *A&A*, 275, 101
- Eggen, O. J., Lynden-Bell, D., & Sandage, A. R. 1962, *ApJ*, 136, 748
- Emsellem E., et al., 2007, *MNRAS*, 379, 401
- Faber, S. M. 1972, *A&A*, 20, 361
- Faber, S. M., & French, H. B. 1980, *ApJ*, 235, 405
- Faber, S. M., Friel, E. D., Burstein, D., & Gaskell, C. M. 1985, *ApJs*, 57, 711
- Falcón-Barroso, J., Peletier, R. F., & Balcells, M. 2002, *MNRAS*, 335, 741
- Falcón-Barroso, J., Bacon, R., Bureau, M., et al. 2006, *MNRAS*, 369, 529
- Falcón-Barroso, J., van de Ven, G., Peletier, R. F., et al. 2011, *MNRAS*, 417, 1787
- Fanelli, M. N., O'Connell, R. W., Burstein, D., & Wu, C.-C. 1992, *ApJs*, 82, 197
- Fazio, G. G., Hora, J. L., Allen, L. E., et al. 2004, *ApJs*, 154, 10
- Ferrarese L., Merritt D., 2000, *ApJ*, 539, L9

- Ferreras, I., La Barbera, F., de Carvalho, R. R., et al. 2012, arXiv:1206.1594
- Förster Schreiber, N. M., Genzel, R., Bouché, N., et al. 2009, ApJ, 706, 1364
- Fulbright, J. P., McWilliam, A., & Rich, R. M. 2007, ApJ, 661, 1152
- Gallart, C., & Leid Team 2007, IAU Symposium, 241, 290
- Ganda, K., Peletier, R. F., McDermid, R. M., et al. 2007, MNRAS, 380, 506
- Gilmore, G., & Reid, N. 1983, MNRAS, 202, 1025
- Giovanelli, R., Haynes, M. P., Salzer, J. J., et al. 1994, AJ, 107, 2036
- Girardi, L., Bressan, A., Bertelli, G., & Chiosi, C. 2000, A&As, 141, 371
- González Delgado, R. M., Cerviño, M., Martins, L. P., Leitherer, C., & Hauschildt, P. H. 2005, MNRAS, 357, 945
- Gorgas, J., Faber, S. M., Burstein, D., et al. 1993, ApJs, 86, 153
- Graves, G. J., & Schiavon, R. P. 2008, ApJs, 177, 446
- Graves, G. J., & Faber, S. M. 2010, ApJ, 717, 803
- Gregg, M. D., Silva, D., Rayner, J., et al. 2006, The 2005 HST Calibration Workshop: Hubble After the Transition to Two-Gyro Mode, p. 209
- Gustafsson, B., Edvardsson, B., Eriksson, K., et al. 2008, A&A, 486, 951
- Hammer, D., Verdoes Kleijn, G., Hoyos, C., et al. 2010, ApJs, 191, 143
- Harris, G. L. H., Harris, W. E., & Poole, G. B. 1999, AJ, 117, 855
- Hauschildt, P. H., Baron, E., & Allard, F. 1997, ApJ, 483, 390
- Hempel, M., Zepf, S., Kundu, A., Geisler, D., & Maccarone, T. J. 2007, ApJ, 661, 768
- Henry, R. B. C., & Worthey, G. 1999, PASP, 111, 919
- Hopkins, P. F., Cox, T. J., Dutta, S. N., et al. 2009, ApJs, 181, 135
- Ibata, R., Irwin, M., Lewis, G., Ferguson, A. M. N., & Tanvir, N. 2001, Nature, 412, 49
- Jones, L. A. 1997, Ph.D. thesis, Univ. North Carolina, Chapel Hill
- Jørgensen I., Franx M., Kjaergaard P., 1992, A&AS, 95, 489
- Kauffmann, G., Heckman, T. M., White, S. D. M., et al. 2003, MNRAS, 341, 54
- Kawata D., Gibson B. K., 2003, MNRAS, 340, 908

- Kennicutt, R. C., Jr. 1999, *ApJ*, 519, 1
- Kobayashi C., 2004, *MNRAS*, 347, 740
- Koleva, M., Prugniel, P., Ocvirk, P., Le Borgne, D., & Soubiran, C. 2008, *MNRAS*, 385, 1998
- Koleva, M., de Rijcke, S., Prugniel, P., Zeilinger, W. W., & Michielsen, D. 2009, *MNRAS*, 396, 2133
- Koleva, M., & Vazdekis, A. 2012, *A&A*, 538, A143
- Kormendy, J., & Kennicutt, R. C., Jr. 2004, *ARAA*, 42, 603
- Kroupa, P. 2001, *MNRAS*, 322, 231
- Kroupa, P. 2007, arXiv:astro-ph/0703124
- Kuntschner H., et al., 2006, *MNRAS*, 369, 497
- Kuntschner H., et al., 2010, *MNRAS*, 408, 97
- Lançon, A., Mouhcine, M., Fioc, M., & Silva, D. 1999, *A&A*, 344, L21
- Lançon, A., & Wood, P. R. 2000, *A&As*, 146, 217
- Lançon, A., & Mouhcine, M. 2002, *A&A*, 393, 167
- Lançon, A., Gallagher, J. S., III, Mouhcine, M., et al. 2008, *A&A*, 486, 165
- Landsman, W., Bohlin, R. C., Neff, S. G., et al. 1998, *AJ*, 116, 789
- Larson R. B., 1974, *MNRAS*, 166, 585
- Le Borgne, D., Rocca-Volmerange, B., Prugniel, P., et al. 2004, *A&A*, 425, 881
- Le Borgne, J.-F., Bruzual, G., Pelló, R., et al. 2003, *A&A*, 402, 433
- Lee, H.-c., Worthey, G., Dotter, A., et al. 2009, *ApJ*, 694, 902
- Leitherer, C., Ortiz Otálvaro, P. A., Bresolin, F., et al. 2010, *ApJs*, 189, 309
- Lejeune, T., Cuisinier, F., & Buser, R. 1997, *A&As*, 125, 229
- Lejeune, T., & Schaerer, D. 2001, *A&A*, 366, 538
- Lyubenova, M., Kuntschner, H., Rejkuba, M., et al. 2012, *A&A*, 543, A75
- Mackey, A. D., Broby Nielsen, P., Ferguson, A. M. N., & Richardson, J. C. 2008, *ApJl*, 681, L17
- Maraston, C. 2005, *MNRAS*, 362, 799
- Maraston, C., Nieves Colmenárez, L., Bender, R., & Thomas, D. 2009, *A&A*, 493, 425

- Marigo P., Girardi L., Bressan A., Groenewegen M. A. T., Silva L., Granato G. L., 2008, *A&A*, 482, 883
- Mármol-Queraltó, E., Cardiel, N., Cenarro, A. J., et al. 2008, *A&A*, 489, 885
- Mármol-Queraltó E., et al., 2009, *ApJ*, 705, L199
- Mateo, M. L. 1998, *ARAA*, 36, 435
- Matteucci, F., & Brocato, E. 1990, *ApJ*, 365, 539
- McConnachie, A. W., Irwin, M. J., Ibata, R. A., et al. 2009, *Nature*, 461, 66
- Meidt, S. E., Schinnerer, E., Knapen, J. H., et al. 2012, *ApJ*, 744, 17
- Michielsen, D., Boselli, A., Conselice, C. J., et al. 2008, *MNRAS*, 385, 1374
- Milone, A. P., Bedin, L. R., Piotto, G., et al. 2008, *ApJ*, 673, 241
- Milone, A. D. C., Sansom, A. E., & Sánchez-Blázquez, P. 2011, *MNRAS*, 414, 1227
- Mouhcine, M., & Lançon, A. 2002, *A&A*, 393, 149
- Norris, J. E., & Da Costa, G. S. 1995, *ApJ*, 447, 680
- O'Connell, R. W. 1980, *ApJ*, 236, 430
- O'Connell, R. W. 1999, *ARAA*, 37, 603
- Ocvirk, P., Peletier, R., & Lançon, A. 2008, *Astronomische Nachrichten*, 329, 980
- Pahre, M. A., de Carvalho, R. R., & Djorgovski, S. G. 1998, *AJ*, 116, 1606
- Panter, B., Heavens, A. F., & Jimenez, R. 2003, *MNRAS*, 343, 1145
- Peletier R. F., 1989, PhD Thesis, University of Groningen
- Peletier, R. F., Valentijn, E. A., Moorwood, A. F. M., et al. 1995, *A&A*, 300, L1
- Peletier, R. F., Balcells, M., Davies, R. L., et al. 1999, *MNRAS*, 310, 703
- Peletier, R. F., Falcón-Barroso, J., Bacon, R., et al. 2007, *MNRAS*, 379, 445
- Peletier, R. 2009, *American Institute of Physics Conference Series*, 1111, 15
- Peletier, R. F., Kutdemir, E., van der Wolk, G., et al. 2012, *MNRAS*, 419, 2031
- Piotto, G., Bedin, L. R., Anderson, J., et al. 2007, *ApJl*, 661, L53
- Piotto, G., De Angeli, F., King, I. R., et al. 2004, *ApJl*, 604, L109

- Pipino, A., D'Ercole, A., Chiappini, C., & Matteucci, F. 2010, *MNRAS*, 407, 1347
- Poggianti, B. M., von der Linden, A., De Lucia, G., et al. 2006, *ApJ*, 642, 188
- Price, J., Phillipps, S., Huxor, A., et al. 2009, *MNRAS*, 397, 1816
- Prugniel, P., Soubiran, C., Koleva, M., & Le Borgne, D. 2007, arXiv:astro-ph/0703658
- Rayner, J. T., Cushing, M. C., & Vacca, W. D. 2009, *ApJs*, 185, 289
- Renzini, A. 2006, *ARAA*, 44, 141
- Ricciardelli, E., Vazdekis, A., Cenarro, A. J., & Falcón-Barroso, J. 2012, *MNRAS*, 424, 172
- Rich, R. M. 1988, *AJ*, 95, 828
- Roberts, M. S. 1963, *ARAA*, 1, 149
- Rodríguez-Merino, L. H., Chavez, M., Bertone, E., & Buzzoni, A. 2005, *ApJ*, 626, 411
- Rose, J. A., Bower, R. G., Caldwell, N., et al. 1994, *AJ*, 108, 2054
- Ryde, N., & Lambert, D. L. 2004, *A&A*, 415, 559
- Saglia, R. P., Sánchez-Blázquez, P., Bender, R., et al. 2010, *A&A*, 524, A6
- Salaris, M., & Cassisi, S. 2006, *Evolution of Stars and Stellar Populations by Maurizio Salaris and Santi Cassisi*. Wiley, 2006. ISBN: 978-0-470-09219-4,
- Salpeter, E. E. 1955, *ApJ*, 121, 161
- Sánchez, S. F., Kennicutt, R. C., Gil de Paz, A., et al. 2012, *A&A*, 538, A8
- Sánchez-Blázquez P., Gorgas J., Cardiel N., 2006, *A&A*, 457, 823
- Sandage, A. 1972, *ApJ*, 176, 21
- Sarzi M., et al., 2006, *MNRAS*, 366, 1151
- Sarzi M., et al., 2010, *MNRAS*, 402, 2187
- Schiavon, R. P. 2007, *ApJs*, 171, 146
- Schiavon, R. P., Barbuy, B., & Bruzual A., G. 2000, *ApJ*, 532, 453
- Scott N., et al., *MNRAS*, 2009, 398, 1835
- Searle, L., Sargent, W. L. W., & Bagnuolo, W. G. 1973, *ApJ*, 179, 427
- Serven, J., Worthey, G., & Briley, M. M. 2005, *ApJ*, 627, 754

- Shapley, H. 1918, *ApJ*, 48, 154
- Silva, D. R., Kuntschner, H., & Lyubenova, M. 2008, *ApJ*, 674, 194
- Smith, R. J., Lucey, J. R., & Carter, D. 2012, *MNRAS*, accepted (arXiv:1206.4311)
- Smith R. J., Lucey J. R., Hudson M. J., Allanson S. P., Bridges T. J., Hornschemeier A. E., Marzke R. O., Miller N. A., 2009, *MNRAS*, 392, 1265
- Spinrad, H., & Taylor, B. J. 1971, *ApJs*, 22, 445
- Spolaor M., Proctor R. N., Forbes D. A., Couch W. J., 2009, *ApJl*, 691, L138
- Terlevich R., Davies R. L., Faber S. M., Burstein D., 1981, *MNRAS*, 196, 381
- Terndrup, D. M. 1988, *AJ*, 96, 884
- Thomas, D., Maraston, C., & Bender, R. 2003, *MNRAS*, 343, 279
- Thomas D., Maraston C., Bender R., Mendes de Oliveira C., 2005, *ApJ*, 621, 673
- Tinsley, B. M. 1968, *ApJ*, 151, 547
- Tinsley, B. M. 1980, *Fund. Cosm. Phys.*, 5, 287
- Tojeiro, R., Heavens, A. F., Jimenez, R., & Panter, B. 2007, *MNRAS*, 381, 1252
- Toloba, E., Boselli, A., Peletier, R.F., Falcón-Barroso, J., van de Ven, G. & Gorgas, J., 2012, submitted to *MNRAS*
- Tolstoy, E., Hill, V., & Tosi, M. 2009, *ARAA*, 47, 371
- Trager, S. C., Faber, S. M., Worthey, G., & González, J. J. 2000, *AJ*, 119, 1645
- Travaglio, C., Gallino, R., Arnone, E., et al. 2004, *ApJ*, 601, 864
- Tremonti, C. A., Heckman, T. M., Kauffmann, G., et al. 2004, *ApJ*, 613, 898
- Valdes, F., Gupta, R., Rose, J. A., Singh, H. P., & Bell, D. J. 2004, *ApJs*, 152, 251
- VandenBerg, D. A. 2000, *ApJs*, 129, 315
- van der Wolk, G., 2011, PhD Thesis, University of Groningen
- van Dokkum, P. G., & Conroy, C. 2010, *Nature*, 468, 940
- van Dokkum, P. G., & Conroy, C. 2011, *ApJl*, 735, L13
- Vazdekis, A. 1999, *ApJ*, 513, 224
- Vazdekis, A., & Arimoto, N. 1999, *ApJ*, 525, 144

- Vazdekis, A., Sánchez-Blázquez, P., Falcón-Barroso, J., et al. 2010, MNRAS, 404, 1639
- Vazdekis, A., Ricciardelli, E., Cenarro, A. J., et al. 2012, MNRAS, 424, 157
- Visvanathan, N., & Sandage, A. 1977, ApJ, 216, 214
- White S. D. M., 1980, MNRAS, 191, 1P
- White, R. E., III, & Keel, W. C. 1992, Nature, 359, 129
- Whitford, A. E. 1975, Galaxies and the Universe, 159
- Whitford, A. E. 1978, ApJ, 226, 777
- Whitford, A. E., & Rich, R. M. 1983, ApJ, 274, 723
- Wolf, J., Martinez, G. D., Bullock, J. S., et al. 2010, MNRAS, 406, 1220
- Worthey G., Faber S. M., Gonzalez J. J., 1992, ApJ, 398, 69
- Worthey, G., & Ottaviani, D. L. 1997, ApJs, 111, 377
- Worthey, G. 1994, ApJs, 95, 107
- Yi, S. K. 2008, Hot Subdwarf Stars and Related Objects, 392, 3
- Yi, S. K., Kim, Y.-C., & Demarque, P. 2003, ApJs, 144, 259
- Zaritsky, D., Gonzalez, A. H., & Zabludoff, A. I. 2006, ApJ, 638, 725
- Zibetti, S., Gallazzi, A., Charlot, S., Pierini, D., & Pasquali, A. 2012, arXiv:1205.4717
- Zinn, R., & West, M. J. 1984, ApJs, 55, 45